Techno-Economic Prospects for Producing Fischer-Tropsch Jet Fuel and Electricity from Lignite and Woody Biomass with CO_2 Capture for EOR

Thomas G. Kreutz[a,d], Eric D. Larson[a,d], Cristina Elsido[b],
Emanuele Martelli[b], Chris Greig[a,c] and Robert H. Williams[a]

[a] Andlinger Center for Energy and the Environment, Princeton University, Princeton, NJ, USA

[b] Department of Energy Politecnico di Milano, Via Lambruschini 4, 20156, Milano, Italy

[c] UQ Energy Initiative and UQ Dow Center for Sustainable Engineering Innovation, University of Queensland, Brisbane, Australia

[d] *corresponding author*

Abstract:

This study explores the prospective techno-economic performance of facilities that produce low- and net-negative-carbon liquid transportation fuels and electricity with CO_2 capture for enhanced oil recovery. The lignite and biomass-to-jet fuel process is based on KBR's TRIG gasifier, Rectisol (for sulfur removal and CO_2 capture), fixed-bed low temperature Fischer-Tropsch synthesis of liquid fuels, and Brayton/Rankine combined cycles to convert synthesis/refining off-gases and waste heat to electricity. This work leverages a recent, highly-detailed assessment of a prospective first-of-a-kind (FOAK) demonstration facility to develop highly detailed Aspen Plus process simulations for nine prospective N^{th}-of-a-kind (NOAK) plant equipment configurations. Component-level capital costs from the FOAK study are scaled and adjusted to reflective prospective learning-by-doing to estimate capital costs for the NOAK designs. NOAK plant economic performance is found to be largely insensitive to variations in plant configurations and electricity output fraction, but biomass input fraction significantly affects profitability. Facilities that consume only carbon-neutral biomass, with no lignite co-feed, have significantly net-*negative* carbon emissions and the most favorable prospective economics when carbon emissions are priced. For these facilities, the crude oil price required for plant economic viability falls rapidly from $100/bbl as carbon emission prices increase above $120/tonne CO_{2eq}. In general, plants that co-fire lignite with biomass are less profitable (than 100% biomass plants) due to their higher net greenhouse gas emissions.

Keywords:

Gasification; Biomass; Carbon negative emissions; Jet fuel; Carbon emission prices; Polygeneration plants

Plant Configurations:

OT	once through
OTA	once through with ATR
RC	syngas recycle
SB	syngas bypass

Plant Design Variables:

f_B	input biomass fraction (HHV)
f_E	output electricity fraction
f_{RC}	syngas recycle fraction
f_{SB}	syngas bypass fraction

Plant Performance Metrics:

BEOP	breakeven (crude) oil price
GHGI	greenhouse gas index
IRR_e	internal rate of return on equity

Abbreviations (variables in italics):

AFUDC	allowance for funds used during construction
AGR	(Rectisol) acid gas removal
AR	as received (feedstock)
ASU	(cryogenic) air separation unit
ATR	(O_2-blown) autothermal reformer
BAU	business-as-usual
bbl_{eq}	barrel of crude oil – energy equivalent
BEC	bare erected (plant) costs
BOP	balance of plant
BTL	biomass-to-liquids plant
CBTL	coal+biomass-to-liquids
CBTLE	coal+biomass-to-liquids+electricity
CCR	(levelized annual) capital charge rate
CCS	CO_2 capture and storage
CI	construction interest
CEPCI	Chemical Engineering Plant Cost Index
CTL	coal-to-liquids
DFBG	dual fluidized bed gasifier
EOR	(CO_2) enhanced oil recovery
EPCM	engineering, procurement, and construction management
EPRI	Electric Power Research Institute
EROI	energy return on investment
EV	(steam) evaporator
FOAK	first-of-a-kind (plant)
FT	Fischer-Tropsch
FTL	Fischer-Tropsch liquids
GHG	greenhouse gas
GT	gas turbine
GTCC	gas turbine combined cycle
HEN	heat exchanger network
HEP	hyperbolic electricity price
HHV	higher heating value
HP	high pressure (steam)
HRSC	heat recovery steam cycle
LBJ	lignite+biomass-to-jet fuel
LCOE	levelized cost of electricity
LHV	lower heating value
LP	low pressure (steam)
LLP	very-low pressure (steam)
LTC	low temperature (syngas) cooling
LTFT	low temperature Fischer-Tropsch
MP	medium pressure (steam)
NETL	U.S. National Energy Technology Laboratory
NOAK	N^{th}-of-a-kind (plant)
OC	owners' costs
O&M	operation and maintenance
p.p.	percentage points
RH	(steam) reheat
SC	(Rankine) steam cycle
SCR	Selective Catalytic Reduction
SG	syngas

SH	(steam) superheat
SPK	synthetic paraffinic kerosene
ST	steam turbine
SWS	sour water stripping (process/unit)
TAG	Technical Assessment Guide
TIT	(gas) turbine inlet temperature
TOT	(gas) turbine outlet temperature
TPC	total (overnight) plant cost
TPI	total plant investment
TRIG	transport integrated gasification
UBAF	upstream biomass accounting factor
USDOE	U.S. Department of Energy
WGS	water-gas shift (reaction/unit)
WSA	wet sulfuric acid (process/unit)
wt.	weight

Individual cases (plant variant) studied here*:

Demo	LBJ demonstration plant
OT-0	OT, *GHGI*=0
OTA-0	OTA, *GHGI*=0
RC-0	RC, *GHGI*=0
OT-1	OT, *GHGI*=1
RC-1	RC, *GHGI*=1
OT-B	OT, 100% biomass
OTA-B	OTA, 100% biomass
RC-B	RC, 100% biomass
SB95-B	OTA, 95% syngas bypass, 100% biomass

* Notation scheme: "***-0***" *GHGI*=0; "***-1***" *GHGI*=1; "***-B***" 100% biomass; all plants except ***Demo*** consume one million tonnes/yr dry biomass (90% plant capacity factor assumed).

1. *Introduction*

Thermochemical conversion of fossil fuels to alternative forms of energy, e.g. electricity, commodity chemicals, hydrogen, ammonia, or liquid transportation fuels, has played a key role in the world's energy economy for more than a century. More recently, the threat of global climate change has catalyzed the development of methods to capture CO_2 in conversion processes for permanent storage in geologic formations ("CO_2 capture and storage", CCS). Because CO_2 capture is impractical on mobile platforms, decarbonizing the transportation sector – which was responsible for ~14% of worldwide greenhouse gas (GHG) emissions and ~23% of total energy-related CO_2 emissions in 2010 [1] – is especially challenging. While the prospect of widespread electrification of transport promises to significantly reduce global GHG emissions via low-carbon sources of electricity to power battery electric vehicles, it is likely that large portions of the sector (e.g. aviation) will continue to be fueled by high energy density liquid hydrocarbon fuels. Energy security is certainly another reason motivating the interest for many coal-rich countries in the development of coal/biomass to synfuels technologies.

Although synthetic gasoline, diesel, and jet fuel (collectively called "synfuels") have been produced commercially for many decades, e.g. via Fischer-Tropsch (FT) synthesis in coal- and gas-to-liquids plants around the globe [2], their system-wide GHG emissions per unit of fuel can be as much as twice that of their petroleum-derived analogs [3]. Adding plant-level CCS can eliminate most non-fuel CO_2 emissions from the synfuels production process, but since synfuels are typically as carbon-intensive as their petroleum-derived analogs, their end use combustion generates comparable amounts of tailpipe CO_2 emissions. This limitation can be overcome by combining CCS with synfuels production from sustainable biomass feedstocks. Because the carbon in biomass is derived from atmospheric CO_2, sustainable biomass production coupled with CO_2 capture during biomass conversion generally leads to *negative* CO_2 emissions. Hence, replacing fossil fuels with sustainable biomass feedstocks – either partially or completely – can reduce system-wide *net* GHG emissions (encompassing fossil fuel extraction, biomass growth and harvesting, the energy conversion facility, underground CO_2 storage, fuel distribution, and synfuels combustion/tailpipe CO_2 emissions) to levels significantly below that of petroleum-derived fuels. As a result, despite the fact that such synfuels are in most other respects virtually equivalent to their petroleum-derived analogs, their unique method of production makes them "low *net* carbon" alternatives.

Coal+biomass-to-liquids+electricity (CBTLE) plants have been studied extensively in the past. For instance, with funding from the U.S. Department of Energy, Larson, et al. [4], Liu, et al. [5] and Williams [6] performed

preliminary design studies to assess the energy, environmental, and economic performance of plants for the co-production of synfuels, chemicals and electricity via co-gasification of coal and biomass. Additional studies focusing on the conversion of coal into liquid fuels were also funded by the U.S. government, included Tarka [7] on the production of diesel from coal and biomass, the National Coal Council [8] focusing on both economic and energy security impacts, Shah et al. [9] investigating coal-to-liquids plants via Fischer-Tropsch Synthesis, and Skone at al. [10] assessing plants for the production of jet fuel via cogasification of coal and biomass using a Transport Reactor Integrated Gasifier (TRIG).

Despite the growing interest and research activity on CBTLE plants, there is limited information regarding actual energy and economic performance, mostly because there are no commercial plants operating today [11] and results are strongly influenced by the modelling and economic assumptions (e.g., performance and costs of selected equipment, plant size, ratio between biomass and coal in the feedstock, type of produced fuels, electricity/fuel output ratio, assumed carbon tax, assumed oil price, etc.). Moreover, there is a large variety of possible plant configurations [12], which makes comparisons of techno-economic performance among different studies challenging. For example, some authors considered co-processing of coal and biomass in a single gasifier [4], while others considered separate coal and biomass gasification trains [5]. Several options are available also for the FT synthesis process: cobalt-based catalyst vs. iron-based catalyst, once-through vs. recycle configurations, and traditional tubular fixed-bed reactors vs. slurry-bed systems [13].

Jiang and Bhattacharyya describe process modelling [14] and techno-economic analysis [15] of a CBTLE plant with CCS. The syngas is produced in a dry-fed (Shell-type) entrained-flow gasifier co-fed with coal and biomass. The plant is designed to produce gasoline and diesel through Fischer-Tropsch synthesis. The fuel synthesis island features autothermal reforming and recycle of unconverted gas. For their base case scenario ("small scale", with biomass-to-coal weight ratio of 8:92 and plant capacity of 10,000 bbl/day) they estimated a thermal conversion efficiency of 45.9% (HHV basis), with 56.9% carbon captured, a specific total investment cost of 870 $/kW of input feedstock (HHV basis) and a break-even oil price between $88/bbl and $106/bbl.

Aitken *et al.* [16] assessed the economics and environmental performance of FT-liquids and electricity obtained from the co-gasification of coal and biomass with carbon capture and storage. A representative CBTLE plant – a composite of plant designs from several studies in the literature – was characterized by 30% biomass input on an energy basis, output fractions equal to 58% diesel, 22% gasoline, and 20% electricity on an energy basis, and 85% carbon capture. Total installed plant cost was about 2000 $/kW of input feedstock. Analysis

performed using the MARKet ALlocation energy model for different potential future scenarios showed that the CBTLE plant scheme was highly competitive in future scenarios with high oil prices and low CCS costs.

Liu et al. [5] compared performance and costs of 16 alternative system configurations that involve gasification-based coproduction of Fischer-Tropsch liquid fuels and electricity from coal and/or biomass, with and without capture and storage of CO_2. The authors considered separate coal and biomass gasification trains, with input biomass accounting for 29-40% of total feedstock HHV inputs. The estimated conversion of feedstock to fuel and to electricity on LHV basis was 31-32% and 13-18%, respectively. Total investment costs were estimated to be 700-900 $/kW of input feedstock (HHV basis).

More recently, a two-part study [17, 18] funded by the U.S. Department of Energy investigates the technical and economic prospects for the production of low-carbon jet fuels from biomass and lignite. The study was informed by inputs from numerous technology vendors and many years of previous research analyzing similar systems. The first part of the study [17] developed a detailed design of a site-specific, first-of-a-kind (FOAK) lignite- and biomass-to- (low-carbon) jet fuel (LBJ) demonstration plant that used KBR's TRIG (Transport Reactor Integrated Gasification) gasifier. The performance of the FOAK plant was modeled in detail using Aspen Plus [19], and comprehensive estimates of its bare-erected capital cost were developed in collaboration with engineers at the WorleyParsons Group. The FOAK analysis [17,18] revealed project economics that were quite unfavorable, partly because of costs associated with the plant's pre-commercial nature, and partly because of its relatively small size (discussed below).

In general, project economics are expected to improve as a result of: 1) scale economies with larger plants, and 2) technological learning that comes with the construction of multiple plants and the maturation of an LBJ industry. To help understand and quantify such improvements, the second part of the study, as reported here, investigated techno-economic prospects for nine different "N^{th}-of-a-kind" (NOAK) variants of the original LBJ demonstration plant, built at commercial scales. It should be noted that the NOAK analysis assumed only the use of technologies that are commercial today, and where technologies from the FOAK design could be scaled up for use in the NOAK designs they were. Future technological innovations may further improve economics, but such considerations were outside the scope of this analysis.

Compared to previous studies available in the literature which report preliminary design studies, this work is based on a detailed design study and costing analysis informed by numerous technology vendors and an experienced engineering and procurement company. The developed design details and cost data are significant features of this paper. As seen in the results, the comprehensive scope of plant design (e.g. we include necessary

auxiliary units neglected in previous studies) and numerous process design constraints ultimately lead to appreciably higher investment cost estimates compared with most of the literature. Additional elements of originality of this work are:

- the investigation and performance comparison of multiple plant designs featuring carbon-positive, carbon-neutral, and carbon-negative emission balances,
- the analysis of plant configurations spanning the full range of electricity/synfuel output ratios,
- the carbon emission balances that consider the fully integrated system from biomass growth and lignite mining to the thermochemical conversion and fuel combustion.

2. *Methodology*

This work seeks to provide a firm quantitative basis for estimating the prospective techno-economic performance of various NOAK plant designs. It adopts commercial process equipment of the same type as used in the FOAK LBJ plant and leverages the FOAK plant's detailed performance model and cost data and, in a structured fashion, investigates the potential commercial prospects of similar CBTLE plants at larger (commercial) scales, assuming prospective NOAK capital costs.

Table 1. Key independent plant design variables and plant performance metrics employed in this study. (See text for details.)

Independent Variables	***Performance Metrics***
Plant configuration	Technical: f_E, η_{FL}
Biomass fraction, f_B	Environmental: $GHGI_{2005}$
Syngas recycle fraction, f_{RC}	Economic: IRR_e, *BEOP*
Syngas bypass fraction, f_{SB}	
Plant scale	

As indicated in Table 1, the "parameter space" of plant design explored here includes different technical designs, feedstock input biomass fraction, f_B (as received, LHV basis), syngas recycle fraction, f_{RC}, syngas bypass fraction, f_{BP}, and plant scale. Technical performance is characterized by: 1) the plant's electricity output fraction, f_E, i.e. the ratio of net output power (MW_e) to net power + Fischer-Tropsch liquids (FTL, MW_{th} LHV). The latter consists of synthetic paraffinic kerosene (SPK) and naphtha:

$$f_E = \frac{net\ electricity\ output}{LHV_{SPK} + LHV_{naphtha} + net\ electricity\ output} \quad (1)$$

and 2) the plant's first law efficiency (LHV basis) in converting "as received" (AR) lignite and biomass to FTL and electricity:

$$\eta_{FL} = \frac{LHV_{SPK} + LHV_{naphtha} + net\ electricity\ output}{LHV_{AR\ lignite} + LHV_{AR\ biomass}} \quad . \quad (2)$$

Similarly, the plant's FTL efficiency (LHV basis) and net electric efficiency (LHV basis) are the separate efficiencies of converting AR lignite and biomass to, respectively, FTL and electricity; their sum is equal to the

plant's first law efficiency (LHV basis). These technical performance metrics vary significantly among the various plant configurations studied here, as described below.

Economies of scale dictate that the specific cost ($ per unit of throughput capacity) of most plant components decreases with increasing scale [20,21]; hence, plant size is a major determinant of prospective profitability. As in previous studies [4,5], we assume that the maximum size of a plant that utilizes biomass is ultimately limited by the amount that can be practically transported by truck to a single site without inducing undue road congestion; the value employed here is a maximum biomass feed rate of 1 Mtonnes/yr (of dry biomass, at 90% capacity factor), or a plant biomass input capacity of ~5,400 AR tonne/day. This constraint, together with GHG emission targets (discussed below), limits the scale of all plants studied here to ~96,000 tonnes/day AR lignite + biomass, or 54,000 bbl_{eq}/day FTL, comparable to the output of a moderately sized crude oil refinery.[1] However, most plants studied here are more than an order of magnitude smaller than this for reasons described below.

A key concern in this project is the plant's carbon footprint, quantified by its net, system-wide GHG emissions:

$$E_{sys} = C_{in}(1 - f_{seq}) - C_{bio}(1 - UBAF) + E_{up} + E_{dwn} \quad (3)$$

where

C_{in} = total carbon content of input biomass and lignite feedstock (kg/s).

f_{seq} = fraction of C_{in} that is captured at the plant and permanently sequestered (dimensionless).

C_{bio} = carbon content of input biomass feedstock (kg/s).

UBAF = upstream biomass accounting factor (dimensionless). *UBAF* accounts for the carbon impact of the way in which the biomass feedstock was grown. *UBAF* can be positive, negative, or zero, as explained below. See [17] for details of how *UBAF* is calculated.

E_{up} = upstream emissions (kg/s) associated with lignite mining and transportation.

E_{dwn} = downstream emissions (kg/s) from synfuels distribution, CO_2 pipeline leakage, and "incremental" EOR operation relative to conventional oil production without EOR. Intermediate coefficients used in estimating E_{up} and E_{dwn} are detailed in Table 2.

[1] To facilitate comparisons on an energy basis, we express FTL output in terms of LHV energy-equivalent barrels of crude oil. Because the volumetric energy density of FTL is lower than that of crude oil, 1 barrel of FTL (actual) corresponds to 0.9 energy-equivalent barrels of crude oil.

Note that the first term in Eq. 3 represents the plant's "primary" system-wide CO_2 emissions, namely direct venting of CO_2 at the plant and synfuels combustion; the second quantifies the potential climate mitigation benefits of growing biomass for use in the plant. For the environmental analysis of the FOAK LBJ demonstration facility, a detailed study of biomass cost and availability around the project site (Meridian, Mississippi) estimated the net biogenic GHG emissions associated with the production of ~600 tonnes/day of pulpwood-quality logs for the process, under various forest management regimens [17]. A *UBAF* value of -0.26 was estimated (for the "moderate" biomass supply option). The negative value means that implementing improved forestry practices (fertilization, thinning, etc.) results in additional growth of biomass relative to a scenario in which no changes in forestry practices are implemented and no biomass is harvested for an LBJ plant, i.e., the counterfactual situation in which the FOAK LBJ project is not built. A *UBAF* of -0.26 means that the amount of biomass grown is 26% more than the amount of biomass fed to the plant; in short, this represents net *carbon-negative* biomass feedstock delivered to the plant.

In contrast to the FOAK LBJ plant, this study explores the *long term* technical, economic, and environmental prospects of commercial CBTLE plants of this type. Our NOAK assumption presumes a future in which the Southeast U.S. is host to many large bioenergy plants, and that a robust biomass supply infrastructure has developed over time. We imagine abundant plantations of woody biomass in this period, where planting occurs almost continuously for the express purpose of regular, future bioenergy harvests. This scenario is better described as a carbon-neutral biomass supply, for which *UBAF*=0 is appropriate. We adopt this assumption here.[2]

Our primary environmental metric is the "greenhouse gas index", $GHGI_{2005}$, the ratio of net system-wide GHG emissions for the given plant, E_{sys}, to those from a comparable reference case:

$$GHGI_{2005} \equiv E_{sys}/E_{ref} \quad (4)$$

where E_{ref} is defined as the full fuel-cycle GHG emissions that would have resulted (on average in the U.S., in 2005) from producing an energy-equivalent mix of petroleum-derived jet and naphtha (from U.S. oil refineries, at 90.7 kg CO_{2eq}/GJ FTL, LHV) and electricity (from the U.S. power grid, at 661 kg CO_{2eq}/MWh) [25].

Table 2. Elements of upstream and downstream GHG emissions, E_{up} and E_{dwn}.

Lignite mining [a]	4.93	[20]
Biomass harvest & transport [a]	3.95	[21]
CO_2 pipeline leakage [b]	0.00683	[22]
Incremental EOR operations [b]	0.0887	[22]

Units: a = kg CO_{2eq}/GJ AR HHV, *b* = kg CO_{2eq}/kg CO_2 delivered

[2] Note: Our choice of *UBAF*=0 effectively neglects "carbon debt" caused by the initial release of bio-carbon to the atmosphere when the original unmanaged forests were first converted to biomass plantations; this is consistent with the assumption of a future mature biomass supply chain, where the carbon debt has been "worked off" by the early-mover bioenergy plants responsible for plantation development.

A reference year of 2005 is used since U.S. national carbon mitigation goals as of 2016 (when the analysis was in progress) were expressed relative to emissions in 2005. For simplicity, $GHGI_{2005}$ is shortened below to *GHGI*. By construction, $GHGI < 1$ indicates that the plant reduces system-wide GHG emissions relative to E_{ref}, $GHGI = 0$ denotes zero net GHG emissions, and $GHGI < 0$ signifies net negative system-wide GHG emissions. In any given CBTLE plant, *GHGI* is governed primarily by its biomass input fraction, f_B, and to a lesser extent the degree of CO_2 capture, both of which vary among the nine plant configurations investigated here.

Key metrics of plant economic viability employed here (Table 1) are: 1) IRR_e, the internal rate of return on invested equity, and 2) the "break-even oil price", *BEOP*, which is the market price for crude oil (without a carbon tax) that yields an IRR_e of 10.2%/yr (discussed below). Our choice of *BEOP* – as opposed to, for example, levelized cost of electricity (*LCOE*) – reflects the project's primary goal of designing an energy conversion facility that can economically produce low-carbon jet fuel. As a result, exogenous market prices are assumed for the primary co-products: electricity, CO_2, and H_2SO_4; revenue from their sale offsets some of the production costs of FTL.

The overarching goal of this work is to identify which NOAK variants of the original LBJ demonstration plant exhibit the most promising technical performance (e.g. high efficiency and low *GHGI*) and economics (e.g. low *BEOP* and high IRR_e). To this end, dozens of plant design variations were constructed in Aspen Plus to span the range of potential biomass input fractions and electricity output fractions – from 0 to 1 for both parameters – as well as further design modifications that govern the extent of CO_2 capture. The technical performance of all plants were simulated in detail, and their economic prospects quantified by calculating: 1) *BEOP* as a function of prospective 20-year levelized CO_2 emissions price, and 2) IRR_e as a function of both crude oil price and CO_2 emissions price. These results reveal the plants' prospective economic competitiveness and the cost to society (quantified by the CO_2 emissions price) required to achieve a given environmental goal (quantified by the *GHGI*).

3. *Description of plant configurations*

Based on knowledge gained from previous techno-economic studies of CBTLE plants [4,5], four distinct plant configurations (shown schematically in Fig. 1) were chosen for close analysis; these are labeled here: 1) "once-through" (OT), 2) "syngas recycle" (RC), 3) "once through with autothermal reforming" (OTA), and 4) "synfuels bypass" (SB). The first three are variations on "light ends" processing, i.e. different ways of handling the H_2- and hydrocarbon-rich offgas streams (often termed "light ends") generated on the synfuels island. The

last option (SB) involves shunting clean syngas around the synfuels island to generate more power in the gas turbine at the expense of FTL production.

Another design parameter investigated here is the biomass/coal fraction, which directly influences the net CO_2 emission balance of the plants. This fraction has been adjusted following three different criteria:

- plants ***OT-0***, ***RC-0***, and ***OTA-0*** achieve a carbon-neutral balance (*GHGI* = 0) considering the integrated system made by biomass growth, harvesting & transport plus conversion that includes capturing most of the carbon entering the plant in the coal and biomass feedstocks.

- plants ***OT-1*** and ***RC-1*** achieve full fuel-cycle GHG emissions equivalent to those when producing and using an energy-equivalent mix of petroleum-derived jet and naphtha with conventional refinery processes (i.e., *GHGI* = 1).

- plants ***OT-B***, ***OTA-B***, ***RC-B*** and ***SB95-B*** use only biomass as input feedstock and as a result produce net carbon negative synfuels (*GHGI* < 0).

3.1 "Once through" (OT) configuration. The OT configuration (also employed in the FOAK LBJ demonstration plant) is a relatively simple design that produces both synfuels and power, but maximizes neither synfuels production nor CO_2 capture. As shown in Fig. 1, sulfur-free syngas from the Rectisol acid gas removal unit (AGR), which has removed sulfur and CO_2 from the syngas, is converted to SPK and naphtha in the synfuels island (comprising the FT synthesis reactor and syncrude refinery); in addition, a multiplicity of refinery light ends (or "offgas") streams are produced, which are compressed, mixed, heated, and finally burned in a gas turbine (GT) to generate electricity. The OT designation indicates that the light ends are directly combusted rather than, e.g. in the RC configuration, reformed to $CO+H_2$ and returned back to the AGR (in an external recycle loop) to increase the yield of synfuels. Note that "once through" is technically a misnomer; in fact, all plants studied here employ a common synfuels island design in which "internal" recycle loops around both the FT synthesis and hydrocracking reactors are used to significantly boost the conversion efficiency of each unit – above their "single pass" values. Although these internal recycle streams were simulated in detail in Aspen Plus, they are neglected in this higher level description of syngas flow through each plant. In the OT configuration only 19.1% of the input feedstock carbon is converted to FTL, roughly

Table 3. Efficiency with which input feedstock energy and carbon are converted in various plant configurations.

Plant Configuration:	***OT-0***	***RC-0***	***OTA-0***
Energy conversion (%, LHV):			
- to synfuels	30.4	40.7	30.5
- to net electric power	13.9	6.9	12.0*
Carbon conversion (%):			
- to carbon in synfuels	19.1	25.6	19.4
- to CO_2 in GT exhaust	20.5	10.6	2.5
- to CO_2 captured for EOR	55.4	58.8	73.1

* Net of power needed to compress N_2 diluent

equal to that vented to the atmosphere from the GT as CO_2 (20.7%); 55.4% is sent away by pipeline as CO_2 for EOR (see Table 3). Regarding energy conversion, 30.4% of the input feedstock LHV is converted to FTL and 13.9% becomes electricity generated by the GT and HRSC.

3.2 Syngas "recycle" (RC) configuration. Relative to the OT configuration, the RC design increases the yield of synfuels – at the expense of net power generation. As depicted in Fig. 1, instead of immediately burning all of the mixed light ends in the GT, they are instead heated, mixed with steam and oxygen, reformed to $CO+H_2$ in an autothermal reformer (ATR), cooled, compressed, and recycled back to the primary syngas stream exiting the plant's primary water-gas shift (WGS) unit, ready for CO_2 capture in the AGR and another

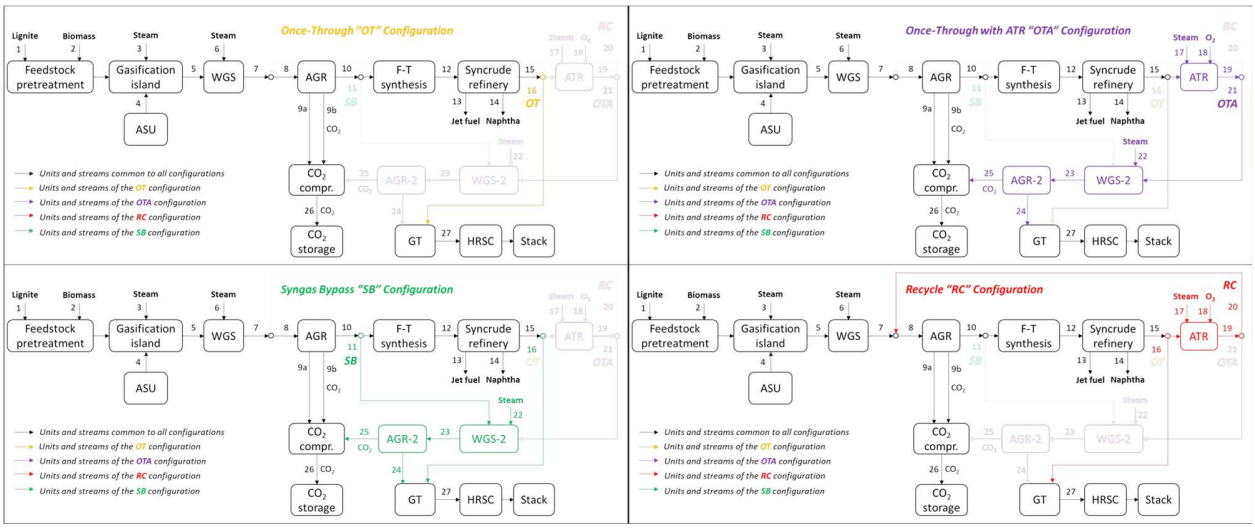

Fig. 1. Schematic of the alternative process designs modelled and analyzed in this work. The scheme shows the main units: feedstock pre-treatment unit (drying, milling), gasification island, water-gas shift (WGS), acid gas removal (AGR), Fischer-Tropsch (F-T) synthesis, syncrude refining, auto-thermal reformer (ATR), gas turbine (GT) and heat recovery steam cycle (HRSC). Components not shown include heat exchangers (syngas coolers and heaters/coolers integrated with the HRSC), sour water stripper (SWS) unit, and wet sulfuric acid (WSA) unit. The Supplementary Material document includes additional process schematics and stream data for numbered streams for all process configurations.

transit through the synfuels island. The fraction of the mixed light ends stream that is recycled, f_{RC}, can vary from zero to 95+%. Zero recycle fraction is equivalent to the OT configuration. As the recycle fraction increases, the synfuels output rises and the plant's net electricity output falls, eventually becoming negative (i.e. the plant must import power to satisfy its parasitic electricity loads). For both conceptual and analytical simplicity, all RC plants in this work are designed with a recycle fraction that yields relatively little (but still positive) net output power, i.e. they produce essentially only FTL and CO_2. For example, as seen in Table 3, in plant ***RC-0*** (f_{RC} = 58.7%), synfuels represent 40.7% of the input feedstock LHV, ~34% higher than in plant ***OT-0***. Although the RC plant's *net* output power is small (by design), it must nevertheless generate ~192 MW_e to

offset its large parasitic power requirements; in contrast to synfuels, net power output represents only 6.9% of the input feedstock.

3.3 "Once through with autothermal reforming" (OTA) configuration. While RC is an OT variant that increases synfuels production, OTA is a configuration designed instead to maximize CO_2 capture. As in RC plants, the light ends are first reformed to CO+H_2 in an ATR; in OTA, however, these gases further undergo secondary WGS to convert most (92.5%) of the CO to CO_2, and secondary AGR to capture the bulk of (96.2%) the CO_2 for EOR. The remaining gas is primarily H_2 (92%) which, after significant N_2 dilution (in order to reduce NO_x formation in the GT combustor and reduce heat transfer to the turbine blades), serves as a low carbon fuel gas for the GT. This configuration reduces CO_2 emissions from the GT exhaust to only 2.5% of the of plant's input carbon; the rest of the CO_2 (in total, 73.1% of the input carbon) is used for EOR. Relative to the OT configuration, the energy and carbon conversion to synfuels are essentially unchanged, but the net electric efficiency falls by ~14% as a result of the additional WGS and CO_2 capture, as well as need for N_2 compression.

3.4 "Synfuels bypass" (SB) configuration. Of the three standard light ends processing designs, the OT configurations yield the highest electricity fractions, 33-36% (LHV basis). Even higher power-to-synfuels ratios can be achieved by utilizing synfuels bypass, in which a fraction of the clean syngas from the AGR is deliberately shunted around the synfuels island. In the SB variant discussed here, the portion of syngas that does not bypass the synfuels island follows the same processing sequence as in the OTA design, rejoining the bypassed stream at the secondary WGS, as shown in Fig. 1.

3.5 Synfuels island details. In the synfuels island, multiple offgas streams from FT synthesis and syncrude refining are heated, compressed, and mixed to create a GT-ready fuel gas at 117°C and 30.3 bara. Its composition, which varies with plant configuration, is primarily CH_4, CO, H_2, and light hydrocarbon gases (below C_6); however, it also contains non-negligible amounts of vaporized, long chain hydrocarbons, C_6-C_{15+}. Detailed stream compositions are provided in the Supplemental Material document. As shown in Fig. 1, this stream (number 15) is processed in various ways, depending on the plant configuration. In OT plants, it is sent directly to the GT. In RC and OTA plants, part of the stream is compressed to 46.4 bara (to account for downstream pressure drops), heated with condensing superheated MP (55 bara, 424.5°C) steam, and mixed with additional steam to provide a 414°C feed gas which is then reformed to synthesis gas in an O_2-blown, Ni-based ATR. The reforming process converts hydrocarbons back to CO and H_2, for either syngas recycle in order to synthesize additional FTL (in RC plants) or for secondary WGS and CO_2 capture for low carbon power generation (in OTA plants). In OTA plants, the ATR reduces the mole fraction of CH_4 from 45.2 to 2.2%; the

remainder is 46.4%vol H_2, 23.2% CO, 21.5% H_2O, and 6.1% CO_2. Following Consonni [26], the ATR's input steam-to-carbon ratio is set to 1.0 and its exit temperature to 1000°C, providing a H_2/CO mole ratio in the reformed syngas of ~2.1; the syngas fraction bypassing the primary WGS unit is adjusted so as to provide a H_2/CO mole ratio of 2.0 in the sweet syngas entering the FT synthesis reactor. In order to avoid metal dusting [27,28], the hot syngas exiting the ATR is first cooled in a medium pressure (MP) steam evaporator (59 bara) followed by a superheater that raises the MP steam temperature to that of the plant's primary MP steam header, 425°C.

In the RC configuration, the reformed syngas is further cooled to 189°C and recycled back to join the main syngas flow. In the OTA configuration, the reformed syngas instead is first cooled to 200°C and mixed with superheated MP steam to yield a 250°C WGS feed with a steam/CO mole ratio of 2.1 (steam/dry exit gas mole ratio = 5.1) [29]. This gas enters a two-stage WGS process (labelled WGS-2 in Fig. 1). It leaves the first (adiabatic, Fe/Cr-based) stage at 403°C with 77.1%vol of its CO converted to $CO_2 + H_2$. This syngas is cooled to 250°C and enters a second (adiabatic, Cu/Zn-based) WGS stage, which increases the total (i.e. two stage) CO molar conversion efficiency to 92.6%. The shifted syngas is then cooled by a series of condensing heat exchangers, followed by a Rectisol CO_2 capture column that extracts 96.2% of the CO_2. The remaining GT fuel gas, which is primarily (92%vol) H_2, contains 83.9% of the lower heating value (LHV) of the original mixed light ends. GT exhaust heat and other process heat sources are converted to electric power in the Rankine-cycle based heat recovery steam cycle (HRSC), described below.

3.6 GT details. In OT and RC configurations, the GT fuel gas is sufficiently similar to natural gas to be burned in a standard dry low-NO_x premixed combustor [30]; in addition, all plants employ downstream selective catalytic reduction (SCR) to reduce NO_x emissions to very low levels. However, OTA (and SB) plants have a GT fuel gas (described above) that is mostly H_2 (92%vol before N_2 dilution). The high flame speed and risk of flashback preclude the use of a premixed combustor; instead, fuel gas dilution and non-premixed combustion are employed. (We assume that no modifications to standard commercial GTs are required, implicitly utilizing the original pressure ratio and expansion nozzle area; only the position of the compressor inlet guide vanes are assumed to change relative to operation on natural gas.) Following [31] and [32], the OTA fuel gas is diluted with compressed N_2 until its stoichiometric flame temperature is 2300 K, which reduces the fuel gas H_2 concentration to 49.7% and lowers the concentration of NO_x in the GT exhaust to ~40 ppmv (down from ~200 ppmv), significantly decreasing the NO_x load on the SCR unit. N_2 dilution also reduces the difference (relative to natural gas) in the fuel's Wobbe index, and lowers the concentration of water vapor in the hot exhaust gases

flowing through the gas turbine expander (from 45.8%vol undiluted to 11.5% with dilution), reducing heat transfer to the turbine blades and thus the rate of their thermal degradation. Following [33], in order to further reduce this relatively high heat transfer and thus achieve blade lifetimes equivalent to those when fueled by natural gas, we additionally derate the turbine inlet temperature (*TIT*) of the GT, somewhat reducing its efficiency. Further details are given in Appendix A, which details our hybrid GT performance model that combines the results of direct simulation in Aspen Plus with a correlation based on the performance of commercial GTs (published in the 2016-17 GTW Handbook, [34]) that captures rising GT efficiency with increasing scale.

3.7 Heat recovery. In the original FOAK LBJ plant design, waste heat was converted to electricity via two separate heat recovery steam cycles (HRSCs), one to cool the GT exhaust (effectively a standard gas turbine combined cycle, GTCC), and the second, custom-designed ("bespoke") HRSC to cool the many process heat streams throughout the plant. This design choice (motivated primarily by operational flexibility considerations, e.g. to facilitate plant startup and allow the GTCC to run as a standalone power generator on natural gas whenever the complex FOAK process train was unavailable) imposes penalties on both the efficiency and cost of waste heat recovery relative to a single HRSC integrating heat from the GT exhaust and process cooling. (See Elsido et al. [35,36] for more details.) In contrast, all NOAK plants studied here employ a single, integrated HRSC. In the comparison between HRSCs for FOAK and NOAK plants reported by Elsido et al. [36], it is shown that for large-scale NOAK plants with high capacity factor adopting an integrated HRSC yields appreciable cost savings and efficiency gains (i.e., net output power) over the "separate HRSC" configuration considered for the FOAK design (i.e., GT HRSC plus distinct process HRSC). Thus, for the NOAK plants considered in this work, only the integrated HRSC configuration has been considered and its performance was separately optimized for each of the nine plant configurations using the constrained energy targeting methodology described in Appendix B.

3.8 Increasing plant scale. Removing the limitation on plant size imposed on the FOAK LBJ plant design (plant scale is constrained here only by our limit of 1 Mtonne/yr of dry biomass input) enables, for example, a roughly 5-fold increase in plant scale for a similarly-configured design. This extension to commercial scales engenders a small number of altered assumptions about plants' technical performance and economics. Guided by [37], the specific power consumption of the ASU at large scales is assumed to drop by 24%, from 461 kWh per short ton pure O_2 (508 kWh/tonne O_2) for the FOAK LBJ demonstration plant to 350 kWh per short ton pure O_2 (386 kWh/tonne O_2). Although the efficiency of other electric motors throughout these plants are generally

expected to rise with increasing plant scale, their specific power consumption was not assumed here to fall with increasing scale. A detailed breakdown of parasitic power loads for each plant is given in Appendix C. Similarly, heat losses from reactors and heat exchangers (as a fraction of their duty) were held fixed. Finally, as described in Appendix A, the efficiency of the GT rises with increasing scale, as noted above.

4. *Performance results*

Technical performance results for all nine plant configurations are given in Table 4. The tenth set of results, labeled ***Demo***, are for the FOAK design from earlier work [17]. For all cases except ***Demo***, the size of all the plant is determined and constrained by the maximum biomass input rate (604 MW_{th} LHV), as discussed above. The primary nine cases are arranged into three groups: three plants with *GHGI*=0, two with *GHGI*=1, and four fed with 100% biomass.[3] The first group, "net carbon neutral" (*GHGI*=0) plants, are all moderately sized (10,000-14,000 tonne/day AR feedstock; 5,300-7,700 bbl_{eq}/day FTL), with biomass input fractions of 35-51%. Their electricity output fractions range from 8.7% (***RC-0***) to 25.1% (***OTA-0***) to 32.8% (***OT-0***); in general, the electricity fractions of all RC, OTA, and OT plants are quite similar to these values. The second, "*GHGI*=1" group are much larger plants (32,000-96,000 tonne/day AR feedstock; 24,000-54,000 bbl_{eq}/day FTL) because the relaxed GHG emissions constraint allows much more lignite to be consumed for a given fixed biomass input;[4] as a result, their biomass input fractions are only 5-15.4%. The third group (100% biomass) are all "carbon-negative" (*GHGI* = -1.1 to -1.7) configurations. They are relatively small plants: 5,400 tonne/day AR biomass.

In general, OT and RC plants are seen (Table 4) to have comparable first law efficiencies: ~45% LHV (for plants with 5-10 thousand tonnes/day AR feedstock). In contrast, the significant additional gas processing (ATR, WGS, and CO_2 capture) in the OTA design exacts a 10-11% (or ~5 percentage points, "p.p.") efficiency penalty. Utilizing 100% biomass is seen to reduce first law efficiencies by 0.2 to 1.0 p.p. relative to lignite+biomass mixtures, due to the higher moisture content of biomass. As discussed above, when comparing case ***Demo*** to ***OT-0***, the reduced ASU specific power consumption and increased GT efficiency when operating at a "commercial" (~5x) scale yields a 16% increase in first law efficiency, from 37.5% to 45.3%. In special

[3] The TRIG gasifier was originally developed for low-rank coals; subsequently, it was shown to work well with mixtures of low-rank coals and biomass. Discussions with engineers involved in the original design, scale-up, and coal+biomass co-processing trials suggest that the technology would be capable of operating on 100% biomass. A variety of other fluidized-bed based gasifier designs have been demonstrated operating using 100% biomass, so this is a plausible claim. Of course testing would be required to verify it.

[4] Plant ***OTA-1*** is omitted here because: 1) it is extraordinarily large, and 2) is not a compelling design, as there is little point in going to such lengths (ATR, WGS, CO_2 capture) to reduce CO_2 emissions in a plant with *GHGI*=1.

case, ***SB95-B***, which generates almost entirely carbon-negative electricity, the first law efficiency is comparatively low, only 33.7%.

Across all plants studied here (except ***SB95-B***), only 18-27% of the input carbon is converted to FTL. OT plants capture the smallest fraction of input carbon as CO_2 (54-57%), RC are intermediate (59%), and OTA capture the most (73-74%). Looking more broadly at the technical performance results in Table 4, we note that, despite the effort made here to design plant variations that have significantly different technical (and economic) performance, the differences between the OT, OTA, and RC configurations are not, in the end, very large. This point will be echoed below in the section on plant economics.

Table 4. Plant configurations and technical performance.

		Carbon-neutral plants:			***GHGI=1 plants:***		***Carbon-negative plants:***			
Plant Configuration:	***Demo***	***OT-0***	***OTA-0***	***RC-0***	***OT-1***	***RC-1***	***OT-B***	***OTA-B***	***RC-B***	***SB95-B***
Recycled syngas fraction, %	-	-	-	58.7	-	63.6	-	-	54.4	-
Syngas bypass fraction, %	-	-	-	-	-	-	-	-	-	95.0
Dry biomass, Mtonne/yr	0.104	1	1	1	1	1	1	1	1	1
Biomass fraction, % LHV	25.0	51.0	35.2	47.9	5.1	15.4	100	100	100	100
Plant Inputs:										
AR lignite, MW_{th} LHV	193	582	1,110	658	11,288	3,326	0	0	0	0
AR biomass, MW_{th} LHV	62.6	604	604	604	604	604	604	604	604	604
Total AR feedstock, tonne/day	2,108	10,034	14,274	10,647	95,995	32,068	5,365	5,365	5,365	5,365
Plant Outputs:										
SPK, MW_{th} LHV	62.6	294.7	426.9	419.8	2,977.2	1,341.3	149.0	149.0	196.3	7.5
Naphtha, MW_{th} LHV	14.0	65.8	95.3	93.7	664.5	299.3	33.3	33.3	43.8	1.7
Total FTL, bbl_{eq}/day	1,128	5,311	7,695	7,567	53,667	24,178	2,687	2,687	3,539	134
GT power output, MW_e	30.5	164.7	216.9	86.8	1,780.7	252.1	83.5	75.5	45.6	186.3
HRSC power, MW_e	22.5†	174.1	251.3	154.1	1,857.7	475.5	88.9	88.6	75.4	115.0
Parasitic power, MW_e	-38.2	-162.6	-293.2	-191.8	-1,593.5	-595.0	-84.7	-106.4	-93.1	-107.0
Net power output, MW_e	*14.8*	*176.2*	*175.1*	*49.1*	*2,044.9*	*132.6*	*87.8*	*57.7*	*28.0*	*194.3*
CO_2 to EOR, tonne/day	1,326	6,318	11,919	7,119	60,152	21,558	3,392	4,455	3,575	5,065
H_2SO_4 (93% wt), tonne/day	49.1	155.4	292.7	175.3	2,938.7	868.9	4.2	4.2	4.2	4.2
Performance Metrics:										
Electricity fraction, % LHV	16.2	32.8	25.1	8.7	36.0	7.5	32.5	24.0	10.4	95.5
El. conv. efficiency, % LHV	5.8	14.9	10.2	3.9	17.2	3.4	14.5	9.5	4.6	32.2
FTL conv. efficiency, % LHV	29.9	30.4	30.5	40.7	30.6	41.7	30.2	30.2	39.7	1.5
First law efficiency, % LHV	35.7	45.3	40.7	44.6	47.8	45.1	44.7	39.7	44.4	33.7
$GHGI_{2005}$ ($UBAF = 0$)*	0.607	0.000	0.000	0.004	0.895	0.856	-1.05	-1.68	-1.35	-1.42
Carbon disposition (% of input):										
In CO_2 vented at plant	22.2	23.4	5.4	13.5	23.7	12.5	23.1	5.4	14.2	12.8
In FTL	19.2	19.1	19.4	25.6	19.9	26.9	18.4	18.4	24.2	0.9
In CO_2 captured for EOR	54.9	55.4	73.1	58.8	54.3	58.5	56.5	74.2	59.5	84.3
In gasifier ash and tar	2.4	2.0	2.0	2.0	2.0	2.0	2.0	2.0	2.0	2.0

* In plant ***Demo***, *UBAF* = -0.26. † In plant ***Demo***, this is the sum of the GT HRSC and "bespoke" HRSC power outputs.

5. *Capital Cost Estimates*

5.1 Bare Erected Costs (*BEC*). Bare-erected capital costs (*BEC*) for individual plant components (except for the GT and HRSC) were scaled from detailed estimates developed in collaboration with engineers at the WorleyParsons Group for the FOAK LBJ demonstration plant [17,18] using component-level power law scaling. The *BEC*, denoted here C (M$), of a plant component having size S, is related to the cost, C_o (M$), of a single train of a reference component with size S_o, by the relationship:

$$C = n^e C_o [S/(n S_o)]^f \quad (5)$$

where n is the integral number of equally sized equipment trains having capacity S/n, f is the component-specific power law cost scaling factor [38], and $e = 0.9$ is the assumed cost scaling exponent for multiple equipment trains.

The component-level capital cost scaling parameters employed here are given in Table 5, where the number of trains for five key plant components (labeled $n_1 - n_5$) are given by:

$$n = \mathrm{INT}(S/S_{max}) + 1 \quad (6)$$

where S_{max} is the largest single train capacity currently employed commercially. The number of trains for many other components is set equal to the most closely related of those five, creating a series of coherent, parallel process trains. Estimates of *BEC* for the GT are given by Eq. A4. For each plant's "bespoke" HRSC, the capital costs of the uninstalled equipment – both HRSC and plant heat exchange network (HEN) – were generated on a plant-by-plant basis using the methods described in Appendix B and multiplied by an installation factor of 1.37 calculated from WorleyParson's detailed capital cost estimate of the LBJ demonstration plant's HRSC [17,18].

It is worth noting that, while the current BEC estimates reported in Table 5 are thought to be reasonably accurate estimates for today's installations, there is an inherent uncertainty in how capital costs of the more specific units (i.e., the gasifier, the synthesis reactor, the refinery island, the acid gas removal process) might evolve over time if LBJ plants become a reference technology. Indeed, thanks to the learning curve in manufacturing and the market competition between vendors, the capital cost of the most specific units could decrease appreciably.

The application of Eq. 5 and Table 5 to each case yields the (partially aggregated) component-level *BEC*s given in Table 6. Additional costs for spare equipment/trains are excluded in this analysis. Economics of scale play an important role in the overall economics of these plants; for example, while case ***OT-0*** is almost five times larger than case ***Demo***, its *BEC* is larger by less than a factor of three.

Table 5. Component-level capital cost scaling parameters (see Eq. 5 and Eq. 6). (2019 US $*).

Plant component(s)	*Scaling parameter*	S_o	S_{max}	n	f	C_o (M$)
Lignite handling	AR lignite, tonne/day	1,366	-	1	0.62	16.1
Lignite milling & drying	AR lignite, tonne/day	1,366	-	$=n_1$	0.66	52.0
Biomass prep. & drying	AR biomass, tonne/day	489.3	-	$=n_1$	0.66	30.9
Feedwater & misc. BOP	AR feed, MW_{th} HHV	259.3	-	$=n_1$	0.713	21.1
Gasifier, SG cooler & aux.	Dried feed, tonne/day	1,281	5,000	n_1	0.64	96.1
ASU & O_2 compression	Pure O_2 output, tonne/day	617.0	3,750	n_2	0.70	66.9
Gas cleanup & piping	AR feed, MW_{th} HHV	259.3	-	$=n_1$	0.725	16.1
Rectisol AGR	Captured CO_2, tonne/day	1,167	8,000	n_3	0.63	96.7
CO_2 drying & compr.	Captured CO_2, tonne/day	1,167	-	$=n_3$	0.67	14.7
WSA unit	H_2SO_4 (93%wt), tonne/day	44.32	-	$=n_3$	0.67	74.5
FT synthesis & refining	FTL output, bbl_{eq}/day	989	70,000	n_4	0.67	15.1
ATR	Syngas output, kmol/hr	31,000	-	$=n_4$	0.67	16.7
WGS reactor	Syngas input, MWth LHV	1,377	-	$=n_4$	0.725	18.5
GT and accessories	GT power, MWe	-	472	n_5	-	Eq. A4
Bespoke HRSC	Calculated case-by-case					
Cooling water system	AR feed, MW_{th} HHV	259.3	-	1	0.598	19.6
Cooling towers	AR feed, MW_{th} HHV	259.3	-	1	0.72	26.9
Ash handling	AR feed, MW_{th} HHV	259.3	-	1	0.64	1.0
Accessory electric plant	Auxiliary power, MW_e	33.65	-	1	0.45	9.0
Main power transformers	Net plant power, MW_e	77.37	-	1	0.71	3.5
Instruments & controls (I&C)	AR feed, MW_{th} HHV	259.3	-	1	0.24	16.9
Other I&C equipment	AR feed, MW_{th} HHV	259.3	-	1	0.13	6.3
Improvements to site	AR feed, MW_{th} HHV	259.3	-	1	0.34	1.9
Buildings & structures	AR feed, MW_{th} HHV	259.3	-	1	0.09	641.1
Steam turbine building	AR feed, MW_{th} HHV	259.3	-	1	0.45	118.0

* Escalated to 2019 US dollars using the Chemical Engineering Plant Cost Index ([39,40]).

Table 6. Disaggregated plant bare erected capital costs, *BEC* (2019 M$), for the cases studied here.

	Demo*	***OT-0***	***OTA-0***	***RC-0***	***OT-1***	***RC-1***	***OT-B***	***OTA-B***	***RC-B***	***SB95-B***
Lignite handling & drying	73.9	172.6	263.0	187.0	1,776.9	645.6	0.0	0.0	0.0	0.0
Biomass handling & drying	33.7	177.5	177.5	177.5	283.1	221.1	150.3	150.3	150.3	150.3
Air Separation Unit (ASU)	73.1	212.6	367.0	284.7	1,672.1	734.6	131.4	153.1	145.7	132.5
Gasifier & ash handling	125.6	393.4	495.4	409.0	2,648.1	1,029.7	222.9	222.9	222.9	222.9
Gas cleanup (AGR, SWS,	138.2	375.3	644.6	402.8	2,878.1	1,125.4	225.9	261.3	232.2	280.3
CO_2 compression	16.5	46.9	84.2	50.9	342.8	137.6	30.9	37.1	32.1	40.5
FT synthesis & refining	81.3	229.6	294.4	291.1	1,081.6	634.0	145.5	145.5	174.9	19.5
Light ends processing	0.0	0.0	84.7	39.3	0.0	89.5	0.0	42.2	22.8	26.9
Gas turbine	15.3	46.8	58.0	28.3	372.1	65.3	27.5	25.4	17.1	51.5
"Bespoke" HRSC+HEN	24.2*	128.5	205.2	141.3	1,327.7	444.3	65.1	71.9	67.4	737.7
Balance of plant (BOP)	106.1	233.9	290.7	243.5	1,025.3	484.6	160.6	164.9	161.9	165.9
Total Plant BEC, M$	*688*	*2,017*	*2,965*	*2,256*	*13,408*	*5,612*	*1,160*	*1,275*	*1,227*	*1,828*

* From [17], where costs were in 2015$. The Chemical Engineering Plant Cost Index was used here to express in 2019$.

5.2 Total Plant Cost (*TPC*). For the FOAK demonstration plant [17], the estimated overnight total plant cost (*TPC*) was based on the *BEC*, with additional anticipated costs for: 1) engineering, procurement and

construction management (EPCM, 20% of *BEC*), 2) process contingencies (35% of *BEC*), and 3) project contingencies (35% of the sum of *BEC* and the preceding costs), yielding a *TPC* of 2.09×*BEC*. Furthermore, based on the research of Greig et al. [41] who studied the detailed history of cost overruns in recent large scale energy projects, for such a complex FOAK plant it was considered prudent to include an additional allowance for "supplementary funds" (20% of preceding *TPC*), yielding an augmented *TPC* of 2.51×*BEC*.

In contrast, for the prospective commercial plants considered here, it is assumed that significant learning has occurred between FOAK and NOAK plant construction. There are very little data on which one might estimate a credible prospective learning rate associated with complex plants of this kind; for expedience and perhaps optimistically, we adopt the assumption that, over time and with sufficient learning: 1) EPCM fees fall to 12% of *BEC*, 2) process contingencies fall to zero (reflecting fully mature processes), 3) project contingencies fall to 10% of *BEC*, 4) supplementary funds are not needed, and 5) *BEC* remains constant over time; the resulting *TPC* equals 1.22×*BEC*. The qualitative rationale for this approach is that: 1) current vender quotes for individual plant components represent the most credible information available about current and future capital costs of equipment, and 2) with the exception of the TRIG gasifier, all components used in these plants are already quite mature. Integration risk is by far the largest uncertainty in constructing such plants, but assuming NOAK conditions implies this risk would also be relatively small.

Table 7. EPRI TAG assumptions and key results.

Debt:equity ratio, %	55:45
Cost of debt, %/yr	4.4 real, 6.5 nominal
Cost of equity, %/yr	10.2 real, 12.4 nominal
Corporate income taxes	39.2 %/yr
Owner's costs (*OC*)	22.8% of *TPC*
Property taxes & insurance	2% of *TPC*+*OC*
Construction time, yr	3, equal annual payments
Book life / tax life, yr	20 / 20
Depreciation schedule	MACRS
Construction interest (*CI*)	7.16% of *TPC*
Capital charge rate (*CCR*)	15.6%/yr of *TPI*

6. *Economic Analysis*

6.1 Approach and financial parameters. Following [33] and [42], our economic analysis employs the frequently used and relatively straightforward EPRI TAG "revenue requirement" methodology [43]; key assumptions and results are summarized in Table 7. A few optimistic (NOAK-inspired) choices bear particular note: 1) a real rate of return on invested equity (or nominal "hurdle rate") of 10.2%/yr[5], 2) a 3 year construction time, with equal annual payments of capital lead to the cost of construction interest (*CI*, also commonly known as "allowance for funds used during construction", *AFUDC*) of 7.16% of *TPC*, and 3) a resulting 20 year

[5] This hurdle rate is the *result* of the EPRI TAG methodology, using the economic assumptions given in Table 7.

levelized capital charge rate (*CCR*) of 15.6%/yr of the total plant investment (*TPI* = *TPC*+*AFUDC*). Fixed and variable operation and maintenance (O&M) costs, calculated by scaling the estimates for the FOAK demonstration plant (detailed in [18]), sum to 5−5.4% of *TPI* per year.

Key assumptions used in the economic analysis are summarized in Table 8. Consonant with the optimistic capital cost assumptions employed above for NOAK projects, the capacity factor for all commercial plants is assumed to be 90%, with no significant ramp-up period required following commissioning. Following [18], the 20 year levelized costs for delivered feedstocks: local (Wilcox Group) Mississippi lignite and southern yellow pine, are 2.14 and 3.70 $/GJ HHV, respectively.[6] Following [44], the plant gate price of CO_2 for EOR, P_{CO_2} ($/tonne), is assumed to change with the market price of crude oil (with no carbon tax), P_{oil} ($/bbl):

$$P_{CO_2} = \lambda P_{oil} - \tau \quad (7)$$

where $\lambda = 0.385$ bbl oil/tonne CO_2, and $\tau = 5$ $/tonne CO_2 is the assumed cost of supercritical pipeline transport from the plant to the EOR site. For example, at a crude oil price of $100/bbl, the plant would receive 33.5 $/tonne for dried CO_2 compressed to 150 bara.

6.2 Coproduct and GHG emissions prices. In the presence of a price on GHG emissions, we assume the plant operator pays for the full lifecycle GHG emissions associated with both the production ("upstream", and at the plant) and consumption (e.g. "downstream" transport, and ultimate combustion of FT products) of its products, primarily FTL and electricity. We assume that the plants studied here, although commercial, are not numerous enough to set prices, but instead act as "market takers" (not "market makers"). As such, market price assumed for each product reflects the average GHG intensity found in the much larger commodities markets. For example, the naphtha and "drop in" FT jet fuel produced by the plant is sold into the market for crude oil-derived analogs whose price is assumed to rise linearly with increasing GHG emission price at a slope equal to the latter's fuel-cycle GHG emissions. Note that, in this economic analysis, no distinction is made between naphtha and SPK jet fuel; we consider only their combined flow, aka FTL.

Electric power is treated in much the same way. Because electricity is a substantial and valuable co-product, revenue from its sale can significantly affect the plant's economics, especially when the electricity output fraction is high. Constructing a general model of the prospective price of wholesale electricity as a function of CO_2

Table 8. Key economic assumptions.

Plant capacity factor	90%
Lignite cost	2.14 $/GJ HHV
Biomass cost	3.70 $/GJ HHV
CO_2 price (plant gate)	Eq. 7
Electricity price	Eq. D1
H_2SO_4 (93% wt) price	133 $/tonne

[6] The estimated marginal price for 8 million tons of pulpwood-quality logs (delivered) is $4.6/GJ HHV ($84/short ton, dry), and for residues is $3.3/GJ HHV ($60/short ton, dry) [23]. A weighted average of the two is employed here.

emissions price is beyond the scope of this study. Instead, we employ a simple "hyperbolic electricity price" (HEP) model designed to capture the dominant features that might appear in a future decarbonized electricity grid: a (carbon-taxed) wholesale price of power that rises with increasing CO_2 emissions price, and then eventually flattens out as the carbon intensity of the grid decreases. The HEP model assumes that, at low CO_2 emission prices, natural gas-fired gas turbine combined cycles (GTCC) are the marginal generator on the dispatch supply stack, and thus set the price of wholesale electricity. As CO_2 emission prices rise, the HEP model assumes that GTCC with post-combustion CO_2 capture and underground storage in a deep saline aquifer (GTCC-CCS) eventually replaces GTCC as the predominant marginal generation technology. This behavior is shown in Fig. 2; the HEP model (red line) assumes that the average wholesale price paid to electricity generators – increasing monotonically over time as a function of rising CO_2 emissions price – is best estimated by a smooth hyperbola that closely fits the two underlying lines of levelized cost of electricity (*LCOE*). The reduced slope of *LCOE* at high GHG emissions price is an important feature of the model; without it, net power generation would be significantly overvalued at very high GHG emissions prices. Details of the HEP model are given in Appendix D.

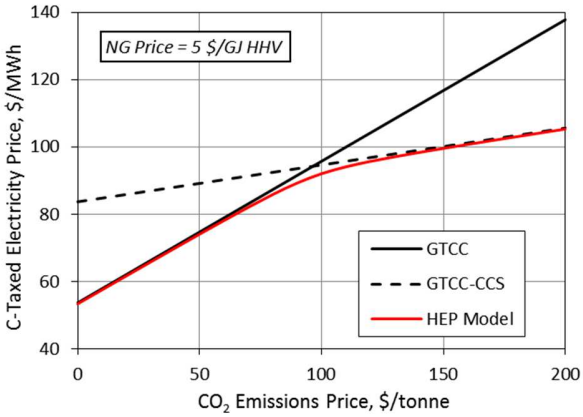

Fig. 2. *LCOE* as a function of CO_2 emissions price for GTCC, GTCC-CCS, and the hyperbolic electricity price (HEP) model. (2019 US$)

6.3 Results

6.3.1 Capital intensity and FTL production cost. The economic performance of selected cases is summarized in Table 9, which details a number of key economic metrics: total plant investment (*TPI*), disaggregated levelized FTL production cost, *BEOP*, and IRR_e – all evaluated at a crude oil price of $50/bbl and a GHG emissions price of $100/tonne CO_{2eq}. The capital intensity of FTL plants is of critical importance. Previous studies (e.g. [3,4,5,6,7,8,9,10]) have found that the specific capital cost of FTL is *much* higher than that of conventional crude oil – the latter is typically in the neighborhood of $10,000/bbl per day – placing FTL plants at a serious competitive disadvantage. The results in Table 9 (for the primary cases) mirror this trend, showing specific capital costs ranging from 325,000 to 620,000 $/bbl per day. Not surprisingly, as a result of scale economics, the largest plants (e.g. those with *GHGI*=1) have the lowest specific cost, while the relatively

small 100% biomass OT and OTA plants (and, of course, plants ***Demo*** and ***SB95-B***) have the largest specific cost.

Table 9. Economic performance (at a GHG emissions price of 100 \$/tonne CO_{2eq}) for various cases investigated here.

		Carbon-neutral plants:			***GHGI=1 plants:***		***Carbon-negative plants:***			
	Demo*	***OT-0***	***OTA-0***	***RC-0***	***OT-1***	***RC-1***	***OT-B***	***OTA-B***	***RC-B***	***SB95-B***
Total Plant Invest. (*TPI*), 2019 M\$	899.4	2,637	3,876	2,949	17,529	7,336	1,517	1,667	1,605	2,390
TPI, \$/bbl per day	797,058	496,513	503,708	389,716	326,629	303,441	564,488	620,284	453,461	17,791,248
FTL Cost Components, 2019 \$/GJ FTL (LHV):										
Installed capital (15.6%/yr of *TPI*)	64.4	40.1	40.7	31.5	26.4	24.5	45.6	50.1	36.6	1.437.3
O&M (at ~5.5%/yr of *TPC*)	21.9	13.0	12.6	9.9	8.6	7.6	15.5	16.3	12.1	417.3
Lignite (at 2.14 \$/GJ, HHV)	6.2	4.0	5.2	3.1	7.6	5.0	0.0	0.0	0.0	0.0
Biomass (at 3.70 \$/GJ, HHV)	3.6	7.3	5.0	5.1	0.7	1.6	14.4	14.4	11.0	288.6
CO_2 emissions (at 100 \$/tonne)	7.5	0.0	0.0	0.0	17.2	8.9	-18.6	-24.7	-14.9	-566.5
CO_2 for EOR (at 44.4 \$/tonne)	-2.9	-2.9	-3.8	-2.3	-2.7	-2.2	-3.1	-4.0	-2.5	-91.7
Output power (at 89.4 \$/MWh)	-4.9	-12.5	-8.6	-2.5	-14.4	-2.1	-12.3	-8.1	-3.0	-546.1
H_2SO_4 (at 133 \$/tonne)	-1.0	-0.7	-0.9	-0.5	-1.2	-0.8	0.0	0.0	0.0	-0.7
Total FTL cost, \$/GJ LHV	94.7	48.3	50.3	44.4	42.1	42.5	41.4	44.0	39.3	938.2
Total FTL cost, \$/gal $gasoline_{eq}$	11.4	5.78	6.03	5.32	5.04	5.09	4.96	5.27	4.71	112.5
BEOP (100 \$/tonne CO_2), \$/bbl_{eq}	341	160	158	151	137	145	131.8	133.2	128.6	395.7
IRR_e (50\$/bbl,100\$/tCO_2), %/yr	0.0	0.0	0.0	0.0	0.0	0.0	0.0	0.0	0.0	0.0

Levelized FTL production costs are the result of an interplay among a host of competing factors. At the simplest level, case ***Demo*** has a specific capital cost that is 58% higher than case ***OT-0***, and twice its resulting FTL cost. All three *GHGI*=0 plants are seen to have similar FTL production costs, 44.4-50.3 \$/GJ LHV (5.3-6.0 \$/gal $gasoline_{eq}$). The two *GHGI*=1 plants exhibit slightly lower FTL costs, ~42 \$/GJ LHV (5 \$/gal $gasoline_{eq}$), because of notably lower specific capital costs (due to increased plant scale) that are almost entirely offset by the cost of their higher emissions (at \$100/tonne CO_{2eq}). This emissions price is seen to favor the 100% biomass plants, whose net FTL production costs are reduced by the GHG emissions revenues that arise from the plants' negative *GHGI*. Revenues from CO_2 for EOR are seen to be fairly significant, reducing the cost of FTL by 5-9%. In OT plants, revenue from output power is more than double to that from CO_2, reducing FTL costs by 20-26%; in OTA plants, the reduction falls to 15%, and in RC plants it is as low as 5-7%. Revenue from H_2SO_4 is generally negligible.

6.3.2 Break-even oil price (*BEOP*). Recall that *BEOP* is the market price for crude oil (in the absence of a carbon tax) that provides the plant operator with a real rate of return on invested equity, IRR_e, of 10.2%/yr (our assumed hurdle rate). *BEOP* is plotted against CO_2 emissions price in Fig. 3 for five plants whose *GHGI* is fixed at either 1 or 0. When *GHGH*=1, *BEOP* is seen to be either flat (for case ***RC-1***) or slightly rising (case ***OT-1***) with increasing GHG emissions price, never falling below ~120 \$/bbl. A flat profile for ***RC-1*** is to be

expected; its output (100% FTL) has the same GHG emissions as crude oil-derived equivalents.[7] Reducing the plants' *GHGI* to 0 (by adding biomass) is seen in Fig. 3 to yield negative slopes as a result of the significantly reduced GHG emissions relative to *GHGI*=1 cases. Case ***RC-0*** is seen to be the most economical of the three plant configurations, by a small degree ($\Delta BEOP$ ~ \$10/bbl). Taken as a whole, the curves in Fig. 3 exhibit an expected result: at low GHG emissions prices, *GHGI*=1 plants are the most economical; at sufficiently high GHG emissions prices, the environmentally superior technology (*GHGI*=0) becomes the more profitable choice.

In Fig. 4, the *BEOP* of plants with 100% biomass, plotted against GHG emissions price, show strikingly different profiles than those in Fig. 3. Despite the fact that these plants have smaller capacities than plants with *GHGI*=0 (Table 4) and thus suffer dis-economies of scale in capital costs, they are nevertheless more economical at GHG emission prices above ~\$90-100/tonne CO_{2eq}. The use of 100% sustainable biomass yields negative *GHGI* values (Table 4), i.e. all these plants scrub significant amounts of CO_2 from the atmosphere. As a result, all curves in Fig. 4 are quite steep, with *BEOP* falling rapidly with increasing GHG emissions price. As in Fig. 3, the OT, OTA, and RC configurations track each other quite closely. At \$100/tonne CO_{2eq}, all three cases are economically viable only when crude oil prices reach 120-130 \$/bbl; at ~\$160-170/tonne CO_{2eq}, they are profitable at oil prices above 50 \$/bbl. The primary product of SB95-B is electricity (Table 4), so more of the input biomass feedstock can be captured than with the other configurations. This leads to the steep slope of SB95-B in Fig. 4.

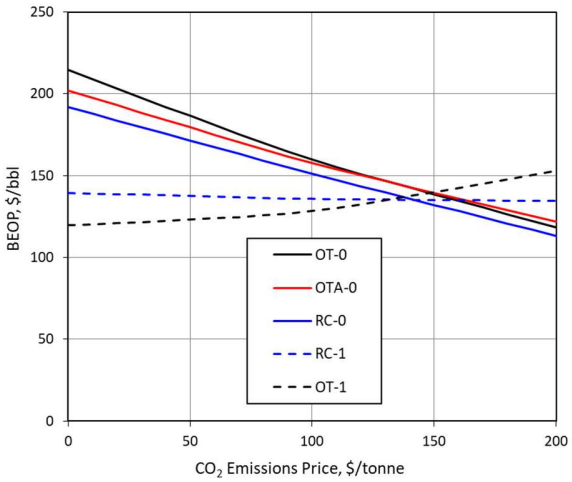

Fig. 3. *BEOP* vs. CO_2 emissions price for plants with *GHGI*=1 and *GHGI*=0.

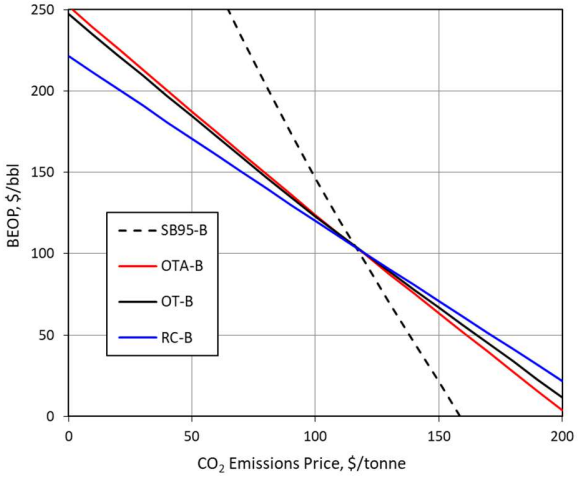

Fig. 4. *BEOP* vs. CO_2 emissions price for (net carbon negative) plants with 100% biomass.

[7] The slightly rising profile of plant ***OT-1*** arises from the fact that its electrical power has (by definition) a carbon intensity equal to that of the reference 2005 U.S. power grid (661 kg CO_{2eq}/MWh), higher than that assumed for the grid in the HEP model (natural gas fired GTCC evolving to GTCC-CCS, i.e. 421 → 110 kg CO_{2eq}/MWh).

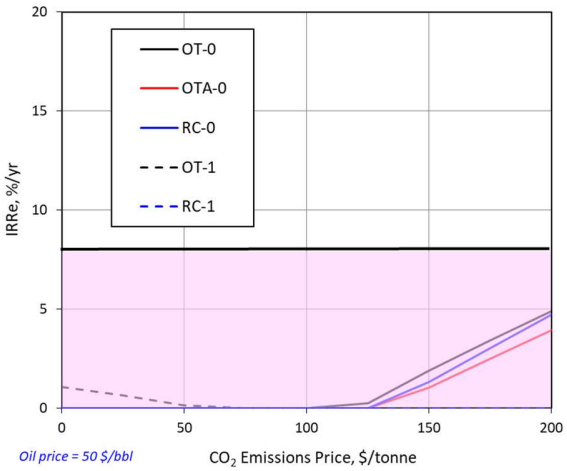

Fig. 5. *IRR*$_e$ vs. CO_2 emissions price for plants with *GHGI*=1 and *GHGI*=0 (crude oil price = \$50/bbl).

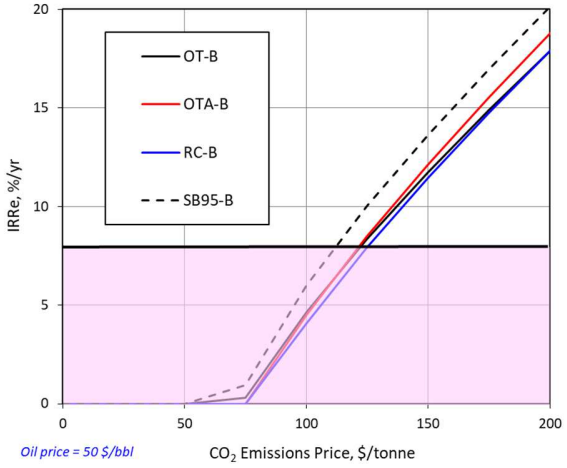

Fig. 6. *IRR*$_e$ vs. CO_2 emissions price for (C-negative) plants with 100% biomass (crude oil price = \$50/bbl).

Note that the three RC cases in Figs. 3 and 4 illustrate the dramatic effect that biomass input fraction has on the sensitivity of plant *BEOP* to GHG emissions price. At the low biomass fraction in case ***RC-1*** (f_B = 15.4%), *BEOP* is ~140 \$/bbl and largely invariant to GHG emissions price. Increasing f_B to 47.9% (carbon neutral case ***RC-0***) causes *BEOP* to fall modestly with increasing GHG emissions price, creating the opportunity for increased profitability above ~\$140/tonne CO_{2eq}. This trend is highlighted in carbon negative case ***RC-B*** (f_B = 100%), whose *BEOP* falls much more quickly with GHG emissions price and is more profitable than ***RC-1*** at emissions prices as low as ~\$/75 tonne CO_{2eq}. In short, in prospective futures that prioritize climate change mitigation, the expectation of significant GHG emissions prices (e.g. above \$100/tonne CO_{2eq}) will drive CBTLE plants to be designed with high input fractions of sustainable biomass.

***6.3.3 IRR*$_e$.** The internal rate of return on invested equity, *IRR*$_e$, is effectively the cost of equity (in EPRI TAG methodology) at which the levelized cost of FTL production equals the (carbon-taxed) price of equivalent crude-oil derived products, i.e. the FTL sale price. *IRR*$_e$ is plotted against CO_2 emissions price in Fig. 5 for the plants whose *GHGI* is fixed at 0 or 1. The figure is consonant with Fig. 3: at an assumed crude oil price of 50 \$/bbl, all plants are economically unviable, i.e. they do not reach the hurdle rate of 10.2 %/yr, at any GHG emissions price across the full range shown in Fig. 5. In Fig. 6, the *IRR*$_e$ of (carbon-negative) plants with 100% biomass are seen to rise rapidly with increasing GHG emissions price (above ~75 \$/tonne CO_{2eq}), and become profitable above ~120 \$/tonne CO_{2eq}. As seen previously in Figs. 3 and 4 (but not readily discerned in Figs. 5 and 6), raising the input biomass fraction increases plant *IRR*$_e$ at high GHG emissions prices.

6.3.4 Electricity fraction. The four 100% biomass plants represent electricity output fractions ranging from 10.4 to 32.5% of the plant's output, and 95.5% for SB95-B, – and yet their IRR_e values in Fig. 6 are almost indistinguishable, except for case SB95-B. This suggests (albeit not conclusively, because other key plant metrics, e.g. *GHGI*, are not constant) that electricity fraction is not a particularly important design variable in the search for maximum plant profitability (or maximum range of economic viability within the parameter space of economic variables we have considered). This result suggests a rough equivalence in the value of the plants' two primary plant co-products, FTL and electricity, that are governed by our assumed crude oil price ($50/bbl) and the HEP model (using a natural gas price of $5/GJ HHV), respectively. Different choices may affect the relative values of the products and thus elevate (or diminish) the importance of the electricity output fraction.

6.3.5 Sensitivity analysis. Our analysis indicates that case ***OT-B*** is one of the most attractive of all NOAK plant variants studied here; it has significantly negative net GHG emissions, is the least complex and least costly of the **–B** configurations, and is also one of the most profitable at high GHG emissions prices. To highlight the sensitivity of IRR_e to the underlying assumed price of crude oil, the IRR_e of case ***OT-B*** is plotted against GHG emissions price for a range of oil prices in Fig. 7. At values as low as 25 $/bbl, the plant is seen to be profitable at ~$170/tonne CO_{2eq}; at 125 $/bbl, economic viability occurs at ~$80/tonne CO_{2eq}. In all cases, the rate of return is seen to rise rapidly with increasing GHG emissions price.

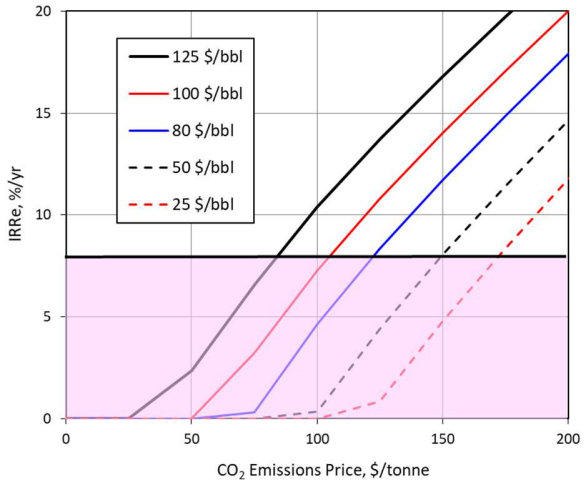

Fig. 7. IRR_e vs. CO_2 emissions price for case ***OT-B***, at various crude oil prices.

In order to quantitatively assess the sensitivity of our two plant economic metrics, *BEOP* and IRR_e, to various important exogenous economic parameters, Table 10 shows how these two metrics change as a result of halving and doubling each parameter. By far the most important is total plant capital cost, *TPC* (also a surrogate for the cost of plant financing, *CCR*), which dramatically affects the plants' prospective economic viability. Fuel and O&M costs are seen to affect profitability less significantly, and natural gas price (which controls the price/value of co-product electricity) and CO_2 value (for EOR) are almost negligible factors.

6.4 Comparison with other NOAK plant designs. It is instructive to compare our NOAK performance and cost estimates with those from studies that have assessed similar process designs. A variety of plant configurations are possible [12], which complicates making meaningful comparisons across studies, but the studies by Liu, *et al*. [5] and Skone, *et al*. [10] have process designs similar enough to those developed in this paper to provide a basis for overall performance comparisons. Liu et al. [5] developed performance estimates for ten distinct process configurations involving separate gasification of coal in a GE Energy slurry-bed reactor and/or biomass in a fluidized-bed reactor, with subsequent combined conditioning of the syngas via water-gas shift and acid gas removal with CO_2 capture before conversion to F-T diesel and gasoline. Electricity is generated by burning the non-condensable gases from the F-T island in a gas turbine combined cycle. Electricity generated in excess of on-side needs is exported from the plant. Skone *et al.* [10] evaluated a system co-processing coal and biomass in a single TRIG gasifier, with subsequent gas processing and integrated CO_2 capture, into a mix of F-T liquid fuels. A small amount of net electricity is exported.

Table 10. Case ***OT-B*** sensitivity analysis: the change in *BEOP* and IRR_e as a result of halving or doubling various exogenous parameters.

	***BEOP* ($/bbl)**		***IRR_e* (%/yr)**	
Base value	137		0.0	
	x 0.5	***x 2***	***x 0.5***	***x 2***
TPC	48	315	10.6	0.0
Fuel cost	110	192	2.9	0.0
O&M	107	197	3.2	0.0
NG price	147	118	0.0	1.8
CO_2 value	160	107	0.0	0.7

Table 11 compares salient overall system performance for six process designs from the present study against similar designs from [5]. The design features used to pair cases between papers were the OT vs. RC nature of the design and the fraction of the input feedstock accounted for by biomass. The fraction of input feedstock energy converted to FT liquids and to electricity are used as the comparative system performance metrics (right-hand three columns in Table 11).

Compared with [5], the fraction of feedstock LHV converted into FT liquids is lower in the present work in all cases, with the largest differences seen for the RC-0 and RC-B cases. Across the matched-pairs of cases, the percentage difference in the fraction converted to FT liquids increases with

Table 11. System performance comparisons with other studies. In each pair of rows, the first and second listed acronyms are for processes from this study and Liu et al. [5], respectively.

	Feedstock		**LHV out/LHV in**		
	MW LHV	**%bio**	**FTL**	**Net elec**	**Total**
OT-0	1,186	0.51	0.304	0.149	0.453
CBTL-OT-CCS [5]	1,566	0.38	0.324	0.164	0.488
OTA-0	1,714	0.35	0.305	0.102	0.407
CBTL-OTA-CCS [5]	2,143	0.28	0.321	0.134	0.454
RC-0	1,262	0.48	0.407	0.039	0.446
CBTL-RC-CCS [5]	1,369	0.44	0.454	0.039	0.493
OT-1	11,893	0.05	0.306	0.172	0.478
CTL-OT-CCS [5]	7,210	0.00	0.313	0.147	0.460
RC-1	3,930	0.15	0.417	0.034	0.451
CTL-RC-CCS [5]	7,559	0.00	0.418	0.039	0.457
RC-B	604	1.00	0.397	0.046	0.444
BTL-RC-CCS [5]	602	1.00	0.475	0.052	0.527

increasing fraction of biomass in the feedstock, reflecting the energy penalty in the present study of processing as-received biomass having a much higher moisture content (43% in the present study compared with 15% in [5]). The feedstock fraction converted to electricity is similar in all cases. This is a result of the level of optimization in heat integration in the two studies: the more significant optimization in this study compensates the suppressive effect on net electricity efficiency of the higher biomass moisture content.

In Fig. 8, total estimated installed capital cost per unit of feedstock input capacity is plotted against input capacity for a large number of plant designs reported in the literature for the production of Fischer-Tropsch liquids from biomass and/or coal. Except for the three estimates for first-of-a-kind plants (FOAK CBTL), most of the other estimates are explicitly or implicitly for N^{th}-of-a-kind plant designs. Two features of this graph stand out: unit capital costs decrease non-linearly with increasing scale, as would be expected, and the variation in cost estimates across relatively narrow ranges of plant sizes is quite large.

Below 1000 MW of feedstock input capacity, most plant estimates fall below the FOAK estimates, as would be expected for NOAK plants. However, the highest NOAK estimate in this narrow capacity range is nearly quadruple the lowest estimate. At larger scales, there is less of a spread in cost estimates, but the variation is still significant where multiple estimates are available. For example for a plant scale of about 6000 MW, the highest cost estimate is more than double the lowest estimate. The estimates made in this paper are in line with the trend observed in Fig. 8. The ***RC-B*** estimate sits at the median value of the plotted BTL estimates. Estimates for the larger ***RC-0*** and ***RC-1*** plants sit above the trend represented by the other plotted estimates.

The wide variation in cost estimates at any given scale suggests that care is required

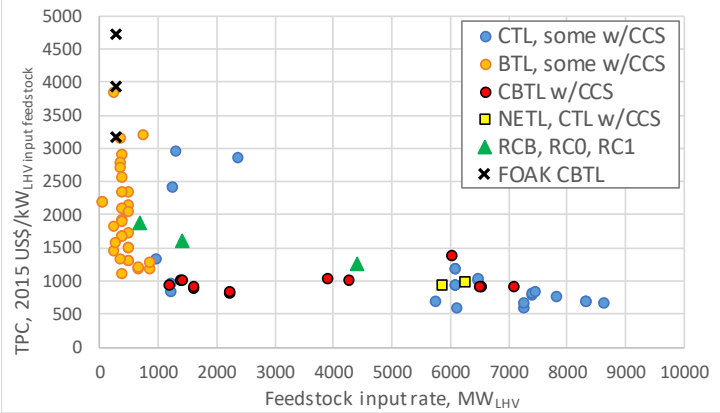

Fig. 8. Compilation of published estimates of total installed capital cost per unit of feedstock input capacity for plants producing Fischer-Tropsch liquids from biomass and/or coal. The plotted points include biomass-to-liquid (BTL) and coal-to-liquid (CTL) plants reported in studies reviewed by Haarlemmer [45],[8] plus some results not included in Haarlemmer's review. The latter include results from two CTL studies by the U.S. National Energy Technology Laboratory (NETL) [9,10], 13 plants co-processing coal and biomass (CBTL) [5,7,15], the ***RC-B***, ***RC-0***, and ***RC-1*** designs reported in this paper, and 3 estimates for a first-of-kind demonstration plant coprocessing lignite and biomass (FOAK CBTLE), as developed by this paper's authors [17].

[8] Harlemmer [45] does not differentiate between plant designs with and without CO_2 capture. Given that all BTL and CTL plants include acid gas removal prior to FT synthesis, the cost difference between plants with and without CO2 capture would be relatively small compared to the uncertainty range implied in Fig. 8.

in interpreting results from any single isolated study. For scoping/pre-feasibility studies of the type included in Fig. 8, comparison of results generated using a self-consistent modeling framework and input assumptions will likely provide more insight than will comparisons of results from studies that use different methodologies and input assumptions.

7. *Discussion and Conclusions*

This study leverages the highly detailed, multi-year, site-specific techno-economic assessment of a prospective first-of-a-kind demonstration facility co-producing synthetic fuels and electricity from biomass and/or lignite [17,18] by significantly extending its extensive Aspen Plus plant model to include nine distinct plant configurations that span a plant design parameter space that includes: biomass input fraction, electricity output fraction, extent of CO_2 capture, and plant scale. Despite the significant range of that parameter space, our analysis reveals that plant economic performance is surprisingly insensitive to the plant configuration, e.g., a "once-through" versus "recycle" design for the fuels synthesis island, and electricity output fraction; only biomass input fraction is found to significantly affect plant economics. Facilities that consume 100% sustainable (carbon-neutral) biomass have the lowest carbon footprint – in fact, all have net carbon-*negative* greenhouse gas emissions – and the most favorable prospective economics in a serious carbon-mitigation policy environment, e.g. in the presence of a significant carbon emission price. None of the plant designs with carbon-positive or carbon-neutral emissions are profitable at crude oil prices below about $120/bbl; only the carbon-negative plants (with only biomass as input) are economically viable at oil prices below $100/bbl, and then only if a carbon emissions price is above $120/tonne CO_{2eq}.

We note the importance of the net carbon emissions of the biomass production system (as characterized in this paper by the upstream biomass accounting factor, *UBAF*), which plays a key role in carbon accounting when substituting biomass for lignite. We explored during the course of this research (but have not presented above) other *UBAF* values. For example, we considered the *UBAF* value of -0.26 estimated for the first-of-a-kind demonstration plant [17]. Such carbon-negative biomass production is extraordinarily effective (per tonne of biomass) in reducing net system greenhouse gas emissions, and hence plants need less biomass to achieve a target carbon footprint. Resulting N^{th}-of-a-kind plant designs with $UBAF < 0$ are often twice the size of those shown here, capturing significant economies of scale. (Recall that plant size is ultimately limited by biomass input.) However, a *UBAF* value of zero is more consistent with a mature future biomass supply chain. This significantly reduces the difference in performance (both technical and economic) between the uneconomic first-of-a-kind plant and the N^{th}-plant variants presented here, rendering the latter less profitable.

A careful comparison with another N^{th}-plant study [5] showed that the fraction of feedstock energy converted into synthetic liquid fuels is lower in the present work in all cases, reflecting an energy penalty of processing as-received biomass having a much higher moisture content (43% in the present study compared with 15% in [5]). In contrast, electricity conversion efficiency is similar between the two sets of studies. This is explained by the heat integration optimization adopted in this study: the added efficiency this provides compensates the negative effect on net electric efficiency of the higher biomass moisture content.

Despite arguably favorable assumptions regarding installed capital costs, the economic prospects of the plants analyzed here are not particularly promising. As seen above (and in previous studies), the specific capital costs ($/bbl) are 10–50 times higher than values typically found in crude oil processing, erecting a very high barrier to adoption. Another fundamental hurdle are large absolute project costs, typically in excess of 1.5 B$, which add to financing challenges. While the large size enables economies of scale, it also involves a high degree of field erection, significantly increasing project complexity and risk.

Future work could address two key open points. First, the type of units (gasifier, acid gas removal unit, etc.) and their designs for the plants explored here were influenced by the limited availability of individual component technology vendors (that were needed to provide accurate performance and cost data). A less restricted unit selection approach may lead to better energy and economic performance. Second, by design only technologies that are commercial today were considered. Advanced technologies under active research and development, but not yet commercial, might improve performance and cost outcomes relative to those reported here.

Declaration of Competing Interest

The authors declare that they have no known competing financial interests or personal relationships that could have appeared to influence the work reported in this paper.

Acknowledgments

This work was undertaken with primary funding from the U.S. Department of Energy's National Energy Technology Laboratory [award number DE-FE0023697]. Southern Company Services and the University of Queensland provided cost-sharing contributions.

Appendix A: Details of Gas Turbine Performance and Cost

The cost and performance of commercial GTs vary significantly with scale. In this work, the extraordinarily wide range of GT outputs – from 45 to 1,780 MW_e – necessitates cost and performance models that accurately capture these variations. This was accomplished by combining: 1) direct simulation in Aspen Plus [19], and 2) published performance data on commercial simple cycle GTs. The former ensures that the models accurately reflect the effects of non-standard operation such as firing with fuel gas whose composition is quite different from natural gas, e.g. the H_2-rich fuel gas of OTA configurations, in which N_2 diluent is added and the turbine inlet temperature (*TIT*) is reduced to extend turbomachinery lifetime. Combining these results with published commercial GT performance data on natural gas enables the model to accurately predict the performance of both natural gas- and syngas-fired GTs whose full load power outputs range over more than an order of magnitude.

GT Performance. Performance data on 215 commercial simple cycle (natural gas-fired) GTs taken from GTW [34] were filtered to create a data set that is relevant to this study. From the original data we excluded GTs with:

- release dates before the year 2000 – in light of our focus on prospective plant performance a decade or more into the future,
- pressure ratios greater than 25 – to isolate heavy duty models and exclude most aeroderivatives,
- power outputs less than 40 MW – because they are not needed for this work, and
- turbine outlet temperatures (*TOT*) less than 550°C – consonant with high efficiency GTs of the future.

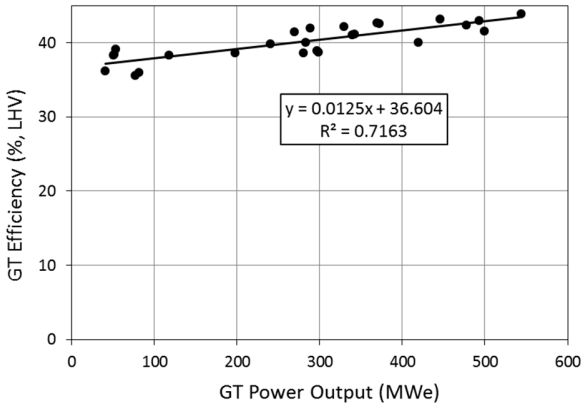

Fig. A1. LHV efficiency of selected commercial GTs operating on natural gas [34].

After this filtering procedure, 26 GT's remained, whose efficiencies and outlet temperatures were regressed as described below.

Gas turbine efficiency (%, LHV), $\eta_{GT}(P)$, is seen in Fig. A1 to increase linearly with power output, P (MW_e). Correspondingly, the GT performance model employed in this work (for operation on natural gas) is:

$$\eta_{GT}(P) = \alpha P + \beta \qquad [P \le 471.7\ MW_e;\ \eta_{GT}(P) \le 42.5\%] \qquad (A1)$$

where $\alpha = 0.0125$ %/MW_e and $\beta = 36.604\%$. Given our focus on future (NOAK) plant performance, rather than restricting plant size to only those particular values where the power output matches that of today's commercial units (or combinations thereof), we instead employ the "continuously variable" assumption in which future GTs

are assumed to be available at *any* given power output with an efficiency given by Eq. A1. In order to prevent GT efficiency from growing to unrealistic values in very large plants, the model's efficiency is capped at 42.5%, the level achieved by GE's 7HA.02, one of the newest and most efficient 60 Hz units on the market today. For computational stability, at output power above 471.7 MW_e, GT efficiency is assumed to remain constant, i.e., the performance model does *not* split the GT into multiple, smaller, less efficient GTs.[9]

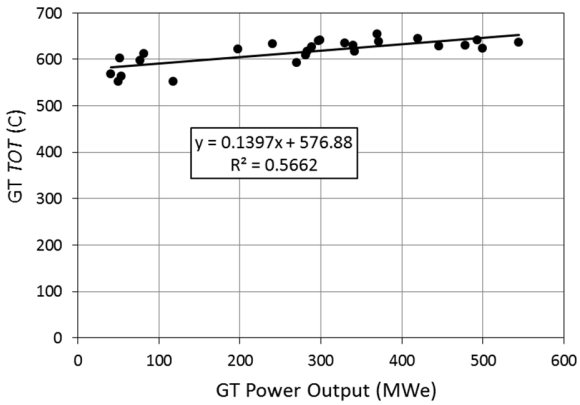

Fig. A2. Turbine outlet temperature (*TOT*) of selected commercial GTs operating on natural gas [34].

As described in [17], the stream of "mixed light ends" from the synfuels island comprises dozens of light hydrocarbon gases. Each plant's configuration – OT, RC, or OTA – dictates how this stream is processed and ultimately the composition of the resulting GT fuel gas. Detailed modeling in Aspen Plus indicates that in OT and RC plants GT performance is virtually identical when fired with (equal LHV flows of) either natural gas or these "mixed light ends". However, the composition of the decarbonized GT fuel gas in OTA (and SB) plant configurations is quite different, containing 92%vol H_2. As a result, we employ non-premixed combustion to prevent flashback and N_2 dilution to reduce NO_x formation. In addition, because H_2-rich fuel gas yields a steam-laden turbine flow whose relatively high heat transfer coefficient reduces turbine blade lifetimes, following [33] we additionally derate the GT's turbine inlet temperature (*TIT*) in OTA and SB plants. After first considering the method of [31], which reduces the *TIT* by ~35°C until critical blade temperatures obtained during H_2-rich syngas operation equal those when firing on natural gas (using the same air cooling flows), we instead adopted the more conservative correlation of Oluyede [46]:

$$\Delta T_{TIT}\,(°F) = 13.312\ \Phi_{H_2}^{0.69} \qquad \text{(A2)}$$

where ΔT_{TIT} is the reduction in *TIT* (°F) and Φ_{H_2} is volume percentage of H_2 (49.7% in case OTA) in the diluted syngas fed to the GT combustor. In case OTA, this correlation derates the *TIT* by 109°C, reducing GT output power by 2.6%. However, relative to operation on (an equal LHV flow of) natural gas, and the GT output power is *increased* by 8.6% as a result of the compressed N_2 diluent which reduces the mass flow of air through

[9] In contrast, our GT capital cost model *does* assume a maximum GT size, above which multiple trains of smaller units are assumed.

the compressor by a comparable amount. As a result, for OTA and SB plants, $\eta_{GT}(P)$ in Eq. A1 is increased by 8.6%.[10]

The turbine output temperatures (*TOTs*) of the commercial GTs described above, needed for optimizing each plant's HRSC, is also seen in Fig. A2 to rise linearly with increasing power. Our model:

$$TOT(P) = \gamma P + \delta \qquad [TOT(P) \leq 642.8°C] \qquad \text{(A3)}$$

where γ= 0.1397 °C/MW$_e$ and δ= 576.88°C, is similarly limited (to 642.8°C, at 471.7 MW$_e$).

GT Capital Cost. The extensive price and performance data on commercial GTs and GTCCs in GTW [34] allows for the construction of a useful capital cost correlation. In Fig. A3, the price of commercial GTs, C_{GT} (2019 \$/kW$_e$), shown as a function of output power, P (MW$_e$), are seen to be well approximated by the following power law relation:

$$C_{GT} = 859.71\ P^{-0.217} \qquad \text{(A4)}$$

Note that the original 2012 cost data were escalated to 2019 U.S. dollars using a CEPCI cost escalation factor of 1.0392 [39; 40]. For simplicity, we use Eq. A4 for all GTs, regardless of fuel gas composition.

Appendix B: Details of Bespoke HRSC Performance

The methodology used in this work to optimize the heat integration and determine a preliminary assessment of the net electric power generated by the heat recovery steam cycle is based on the method of Marechal and Kalitventzeff [47,48] integrated with the "*p-h* superstructure" for Rankine cycle recently proposed by [49]. Given the following data:

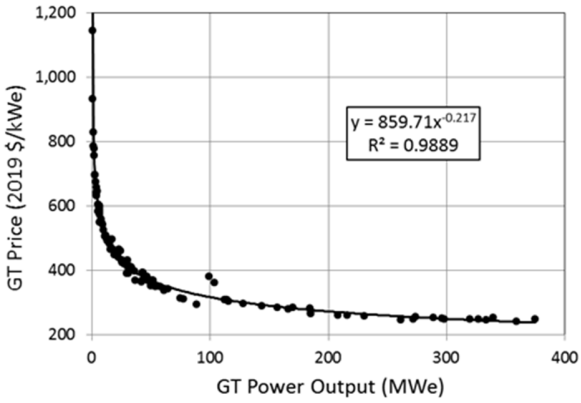

Fig. A3. Price of commercial GTs as a function of output power [34].

- the set of hot and cold streams of the plant and their inlet/outlet temperatures and flow heat capacities,
- the set of hot and cold utility systems (e.g., boilers, cooling water, etc.) and the "*p-h* superstructure" containing all the possible configurations of the heat recovery steam cycle,

[10] After subtracting the power needed for N_2 compression (from a high pressure ASU, at 234.3 kJ/kg N_2), the *net* power output is only 2.7% higher than the output of the GT fired with natural gas. Note that, in this work, differently from [17] which considers a low pressure ASU, the power used to compress N_2 diluent is ~40% lower.

- the set of hot and cold streams of each utility system (including heat recovery steam cycle) and their inlet/outlet temperatures, specific heat capacities and specific energy consumption/production,
- the heat recovery approach temperature contributions for each hot/cold process and utility stream,
- the set of forbidden and forced matches between hot and cold process streams and utility streams,

the methodology determines the optimal selection of the utility systems, their configuration, and the flow rates of each utility stream by maximizing the net electric power generated by the heat recovery steam cycle (i.e. the difference between the power generated by the steam turbine and the power consumption of the feedwater pumps and cooling water circulation pumps).

Note that, in this work, no separate/additional hot utility (i.e. boiler) was considered in order to avoid additional CO_2 emissions. Thus, the heat required by the cold process streams must be either provided by the hot streams or by the steam condensers of the heat recovery steam cycle. Since no extra fuel is burned within the HRSC and HEN, it is worth noting that maximizing the net electric power output is equivalent to maximizing the net electric efficiency of the plant.

The adopted HRSC superstructure is the same used in recent work [36] specifically focused on the optimization of the heat integration, HEN synthesis and HRSC design for the LBJ plants considered in this work. The HRSC superstructure, represented in Fig. B1, was derived by considering the process specifications and the plant's requirement for reaction steam and heat as well as the temperature of its waste heat. It can

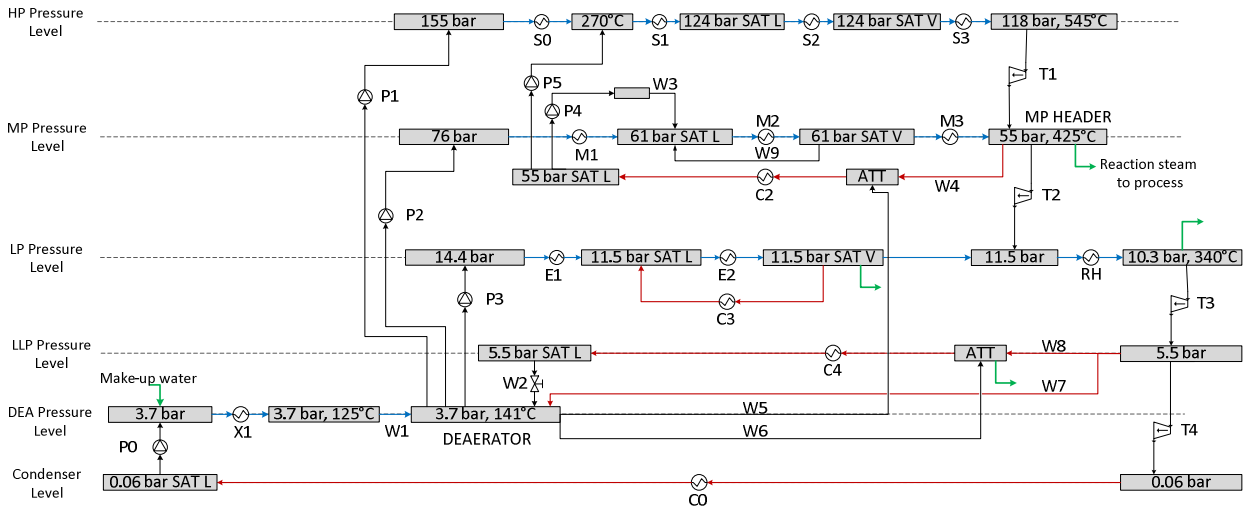

Fig. B1. Scheme of the "*p-h* superstructure" used for representing the possible HRSC configurations. Grey boxes denote steam/water headers (at fixed pressures and temperatures) which are connected by equipment units (pumps, economizers, evaporators, superheaters, valves), as described in [49].

feature up to three pressure levels for steam evaporation, termed high, medium, and low pressure (HP, MP, and LP), and three levels for steam extraction: medium, low and, "low-low" pressure (MP, LP and LLP). The HP level and the MP level must deliver steam to a large MP steam header which provides steam for both the process users (reaction steam for the gasifier, WGS reactor, and syncrude refinery fractionator) and condensing steam heaters (or "condensers"). LP saturated steam for LP condensers can be directly extracted from the LP drum of the evaporator. In addition, an extraction of even lower pressure (LLP) steam from the turbine can be used to satisfy low temperature heat requirements of the process or steam cycle itself. To this end, it is worth noting that, in theory, condensing steam heaters can be matched not only with cold process streams but also with steam cycle economizers to automatically obtain regenerative feedwater preheaters.

Table B1. HRSC assumptions employed here (adapted from [36]).

HP evaporation level, bar	100
MP evaporation level, bar	61.1
LP evaporation level, bar	11.5
MP header, bar	55
LLP extraction header, bar	5.5
Condenser pressure, bar	0.06
HP superheat temperature, °C	500
MP superheat temperature, °C	425
LP superheat/reheat temperature, °C	340
ΔP in feedwater lines, % of EV pressure	20
ΔP in SH steam lines, % of EV pressure	10
Heat loss from all heat exchangers, %	0.5
Isentropic efficiency of HP ST, %	76.1
Isentropic efficiency of MP ST, %	76.1
Isentropic efficiency of LP & LLP STs, %	90
Mechanical/electrical ST efficiency, %	98
Hydraulic pump efficiency, %	80
Mechanical-electrical pump efficiency, %	95

The key cycle parameters for the HRSC assumed in this work are reported in Table B1. The values of pressures and temperatures of the evaporation/extraction levels are directly specified based on the needs of the process as well as techno-economic design constraints. The superheat temperature of HP steam and the pressure of the HP evaporation level were adjusted to have an extraction temperature of 425°C at 55 bar (assuming 90% isentropic efficiency of the HP turbine section), slightly above the minimum steam conditions required by the gasifier. The resulting values are respectively 545°C for the HP superheated steam temperature and 124 bar for the HP evaporation pressure. The MP evaporation pressure was set at 61 bar to yield enough pressure at the exit of the superheater – to match the pressure of the MP steam header. The LP level was set at 11.5 bar, as required by the F-T reactor (whose cooling system uses boiling steam at 11.5 bar), and its superheat temperature was set at 340°C, the minimum value to have enough steam quality at the turbine exit (i.e., above 0.88 – 0.89). The LLP turbine extraction was set at 5 bar (152°C condensation temperature) to accommodate the large heat requirement of the distillation column reboilers in the Rectisol AGR process. The condenser pressure was set at 0.06 bar to guarantee a minimum temperature difference of 5°C with the cooling water.

Following industrial practice, numerous constraints must be explicitly considered in the design optimization problem of the HEN and HRSC, as illustrated in [36]. Among these, the "no stream splitting" constraint and the

rigorous trade-off between efficiency and costs can be considered only by simultaneous optimization methods, such as the ones proposed by [50] and [51]. However, [36] demonstrated that, for relatively large scale NOAK plants featuring mature technologies, the proposed energy targeting methodology is likely to yield HRSC designs and energy performance estimates that are close to those found with the simultaneous techno-economic synthesis methodology [51].

As far as the economic analysis is concerned, the targeting methodology adopted to optimize the heat integration and performance of the HRSC does not allow estimating the capital cost of the heat exchangers because the HEN is not modelled explicitly. Thus, the total bare erected capital cost (BEC) has been estimated using a simplified approach based on the observation that the LBJ NOAK plants considered in this work are expected to share a HRSC and HEN similar to those of the LBJ NOAK plant considered in [36]. For the present work, therefore, we estimate the capital cost of the HEN and HRSC per kW_{th} of heat recovered to be the same as for the HEN and HRSC of the NOAK plant in [36].

Appendix C: Details of Parasitic Electric Loads

Table C1. Parasitic electric loads (kWe) for plant configurations investigated here.

Plant Configuration:	***Demo***	***OT-0***	***OTA-0***	***RC-0***	***OT-1***	***RC-1***	***OT-B***	***OTA-B***	***RC-B***	***SB95-B***
Lignite handling and drying	2,978	8,960	17,097	10,136	173,925	51,246	0	0	0	0
Biomass handling and drying	1,070	10,329	10,329	10,329	10,329	10,329	10,329	10,329	10,329	10,329
ASU O_2 produc. (to 51.7 bara)	14,832	51,793	92,649	64,468	526,105	204,827	26,030	32,397	30,189	26,348
Gasifier and syngas scrubber	30	139	200	148	1,377	457	72	72	72	72
Acid gas removal (AGR)	5,178	24,667	46,539	27,795	234,862	84,173	13,245	17,394	13,958	19,777
Sour water stripper (SWS)	17	81	116	86	798	265	42	42	42	42
CO_2 compression to 150 bara	6,838	32,576	61,461	36,708	310,168	111,162	17,492	22,971	18,434	26,118
WSA unit	115	364	685	410	6,875	2,033	10	10	10	10
H_2 recovery for hydrocracking	127	597	865	851	6,032	2,718	302	302	398	15
FT refining compr. & pumps	765	3,600	5,216	5,128	36,368	16,383	1,820	1,820	2,398	91
Light ends compressor	0	0	1,638	913	0	3,160	0	584	398	29
Light ends processing (SB)	0	0	0	0	0	0	0	0	0	1,051
GT fuel gas compressor	1,544	7,949	11,455	10,862	78,820	34,667	4,088	4,088	5,114	204
N_2 compressor	0	0	11,793	0	0	0	0	4,283	0	10,220
Tempered water system	79	370	533	394	3,666	1,215	191	191	191	191
Cooling water system	2,051	8,702	13,857	9,385	81,849	28,458	4,589	5,110	4,633	5,889
Water treatment	465	2,402	3,909	3,082	23,395	9,581	1,264	1,435	1,500	1,337
Wastewater treatment	390	2,013	3,277	2,583	19,611	8,031	1,059	1,202	1,258	1,121
Misc. low voltage users	1,717	8,018	11,537	8,527	79,361	26,305	4,143	4,143	4,143	4,143
Total power consumption	*38,197*	*162,558*	*293,156*	*191,804*	*1,593,542*	*595,008*	*84,675*	*106,373*	*93,067*	*106,987*

Appendix D: Details of the hyperbolic electricity price (HEP) model

As described above, the HEP model assumes that natural gas GTCC and GTCC-CCS are the marginal power generators – at low and high GHG emission prices, respectively – and thus are entirely responsible for setting wholesale electricity prices in these two regimes. Rather than employ the short run marginal cost (i.e. operating cost) of each plant plus a capacity payment, for simplicity we use instead their levelized long run marginal cost (i.e. operating + capital costs), which should more accurately reflect the true equilibrium cost of power generation from these technologies. The levelized cost of electricity (*LCOE*, 2019 $/MWh) for each plant is calculated using the EPRI TAG model described above, applied to the performance and capital cost data for both technologies in NETL [52] (escalated to 2019$ via the CEPCI), using an assumed wholesale natural gas price of 5 $/GJ HHV. As seen in Fig. 2, since *LCOE* rises linearly with CO_2 emission price, it is sufficient to specify for each generator the value at zero CO_2 emission price, P_n ($/MWh), and the carbon intensity of the power, θ_n (tonne CO_{2eq}/MWh), where subscript n=1 indicates GTCC and n=2 denotes GTCC-CCS; these are listed in Table D1. The HEP model (red line in Fig. 2) assumes that the average wholesale price paid to electricity generators, P_{HEP} ($/MWh) – rising over time, as a function of rising CO_2 emission price – is best estimated by a smooth hyperbola that closely fits the two underlying lines of *LCOE* vs. CO_2 emissions price, P_{CO2} ($/tonne CO_2). Computationally, this is achieved by the simple mathematical formalism of [53]:

$$P_{HEP} = \beta_0 + \beta_1(P_{CO2} - P_0) + \beta_2\sqrt{(P_{CO2} - P_0)^2 + \delta^2/4} \quad \text{(D1)}$$

where

$$\beta_0 = P_1 + \theta_1 x_0 \quad \text{(D2)}$$

$$P_0 = (P_2 - P_1)/(\theta_1 - \theta_2) \quad \text{(D3)}$$

$$\beta_1 = (\theta_1 + \theta_2) / 2 \quad \text{(D4)}$$

$$\beta_2 = (\theta_2 - \theta_1) / 2 \quad \text{(D5)}$$

and $\delta = 40$ is the "curvature parameter" that governs how closely the hyperbola matches the two lines.

Table D1. HEP model parameters. (2019 US$)

	n	P_n ($/MWh)	θ_n (tonne CO_{2eq}/MWh)
GTCC	1	53.8	0.421
GTCC-CCS	2	83.7	0.110

References

[1] IPCC, 2014. "Climate Change 2014: Mitigation of Climate Change", Contribution of Working Group III to the Fifth Assessment Report of the Intergovernmental Panel on Climate Change [Edenhofer, O., R. Pichs-Madruga, Y. Sokona, E. Farahani, S. Kadner, K. Seyboth, A. Adler, I. Baum, S. Brunner, P. Eickemeier, B. Kriemann, J. Savolainen, S. Schlömer, C. von Stechow, T. Zwickel and J.C. Minx (eds.)]. Cambridge University Press, Cambridge, United Kingdom and New York, NY, USA.

[2] Arno de Klerk, 2011. "Fischer–Tropsch Refining", Wiley-VCH Verlag & Co., Weinheim, DE.

[3] National Research Council, 2009. "America's Energy Futures Panel on Alternative Liquid Transportation Fuels, Liquid Transportation Fuels from Coal and Biomass: Technological Status, Costs, and Environmental Impacts".

[4] E.D. Larson, R.H. Williams, and T.G. Kreutz, 2012. "Energy, Environmental, and Economic Analyses of Design Concepts for the Co-Production of Fuels and Chemicals with Electricity via Co-Gasification of Coal and Biomass", final report to DOE NETL under DE-FE0005373,30 June.

[5] G. Liu, E.D. Larson, R.H. Williams, T.G. Kreutz, and X. Guo, 2011. "Making Fischer-Tropsch Fuels and Electricity from Coal and Biomass: Performance and Cost Analysis", *Energy & Fuels*, **25**(1), 415-437.

[6] R.H. Williams, 2013. "Coal/biomass coprocessing strategy to enable a thriving coal industry in a carbon-constrained world", *Cornerstone*, **1**(1): 51-59.

[7] T.J. Tarka, 2009. "Affordable, Low-Carbon Diesel Fuel from Domestic Coal and Biomass", DOE/NETL-2009/1349, National Energy Technology Laboratory.

[8] National Coal Council, 2012. "Harnessing Coal's Carbon Content to Advance the Economy, Environment, and Energy Security", Washington, DC.

[9] V. Shah, N.J. Kuehn, M.J. Turner, and S.J. Kramer, 2014. "Cost and Performance Baseline for Fossil Energy Plants, Vol 4: Coal-to-Liquids via Fischer-Tropsch Synthesis", DOE/NETL-2011/1477.

[10] T. Skone, T. Eckard, J. Marriott, G. Cooney, J. Littlefield, C. White, D. Gray, J. Plunkett, and W. Smith, 2014. "Comprehensive Analysis of Coal and Biomass Conversion to Jet Fuel: Oxygen Blown, Transport Reactor Integrated Gasifier (TRIG) and Fischer-Tropsch (F-T) Catalyst Configurations", DOE/NETL-2012/1563.

[11] G. Liu, B. Yan, and G. Chen, 2013. "Technical review on jet fuel production", Renewable and Sustainable Energy Reviews, 25, 57-90.

[12] A.M. Niziolek, O. Onel, J.A. Elia, R.C. Baliban, X. Xiao, and C.A. Floudas, 2014. "Coal and Biomass to Liquid Transportation Fuels: Process Synthesis and Global Optimization Strategies", *Industrial & Engineering Chemistry Research*, **53**, 17002−17025.

[13] S.S Ail, and S. Dasappa, 2016. "Biomass to liquid transportation fuel via Fischer Tropsch synthesis – Technology review and current scenario", *Renewable and Sustainable Energy Reviews*, **58**(C), 267-286.

[14] Y. Jiang, and D. Bhattacharyya, 2014. "Plant-wide modeling of an indirect coal–biomass to liquids (CBTL) plant with CO2 capture and storage (CCS)", *International Journal of Greenhouse Gas Control*, **31**, 1-15.

[15] Y. Jiang, and D. Bhattacharyya, 2016. "Techno-Economic Analysis of a Novel Indirect Coal−Biomass to Liquids Plant Integrated with a Combined Cycle Plant and CO2 Capture and Storage", *Industrial & Engineering Chemistry Research*, **55**, 1677−1689.

[16] M.L. Aitken, D.H. Loughlin, R.S. Dodder, and W.H. Yelverton, 2016. "Economic and environmental evaluation of coal-and-biomass-to-liquids-and-electricity plants equipped with carbon capture and storage", *Clean Technologies and Environmental Policy*, **18**, 573-581.

[17] E.D. Larson, T.G. Kreutz, C. Greig, R.H. Williams, T. Rooney, E. Gray, C. Elsido, E. Martelli, and J.C. Meerman, 2020. "Design and Analysis of a Low-Carbon Lignite/Biomass-to-Jet Fuel Demonstration Project", *Applied Energy*, **260**, 114209.

[18] C. Greig, T.G. Kreutz, E.D. Larson, J.C. Meerman, and R.H. Williams, 2017. "Lignite-plus-Biomass to Synthetic Jet Fuel with CO2 Capture and Storage: Design, Cost, and Greenhouse Gas Emissions Analysis for a Near-Term First-of-a-Kind Demonstration Project and Prospective Future Commercial Plants," Final report for Project #DE-FE0023697 to The National Energy Technology Laboratory, U.S. Department of Energy.

[19] AspenTech, 2015. Aspen Plus chemical process simulation software, version 8.6.

[20] D.L. Phung, "Theory and Evidence for Using the Economy-of-Scale Law in Power Plant Economics," ORNL/TM 10195, Oak Ridget National Laboratory, Oak Ridge, TN, USA, May 1987.

[21] Turton, R., Shaeiwitz, J.A., Bhattacharyya, D., and Whiting, W.B., Analysis, Synthesis, and Design of Chemical Processes, 5th Ed., Pearson Education Inc., 2018.

[22] P. Pietro, 2010. "Life Cycle Analysis of Coal and Natural Gas-fired Power Plants", presented at EPRI Coal Fleet.

[23] T. Rooney, and E. Gray, 2016. "Biomass Supply and Biogenic Carbon Impacts Evaluation for Lignite-Biomass to Jet Fuel Project, Final Report," Antares Group Inc.

[24] Air Force Research Laboratory, 2011. *Advanced Alternative Energy Technologies, Subtask: Life Cycle Greenhouse Gas Analysis of Advanced Jet Propulsion Fuels: Fischer-Tropsch Based SPK-1 Case Study*, The Aviation Fuel Life Cycle Assessment Working Group, Final Report, (Rapid Response R&D for the Propulsion Directorate, Delivery Order 0019, RL-RZ-WP-TR-2011-2138), AFRL Propulsion Directorate, Wright-Patterson AFB, Ohio.

[25] GREET, 2015. "The Greenhouse Gases, Regulated Emissions, and Energy Use in Transportation Model," Argonne National Laboratory. https://greet.es.anl.gov/

[26] S. Consonni and F. Vigano, 2005. "Decarbonized hydrogen and electricity from natural gas", *International Journal of Hydrogen Energy*, **30** 701–718.

[27] H.J. Grabke, R. Krajak, and E.M. Müller-Lorenz, 1993. "Metal dusting of high temperature alloys", *Werkstoffe und Korrosion* **44**(3), 89–97.

[28] H.J. Grabke, and M. Spiegel, 2003. "Occurrence of metal dusting – referring to failure cases", *Materials and Corrosion* **54**(10), 799–804.

[29] Haldor Topsoe, 2016. Personal communication with Livia Sierra Llorens, Haldor Topsoe Inc.

[30] Siemens, 2015. Personal communication from Clement Celestin, Siemens AG to Harvey Goldstein, WorleyParsons, Ltd.

[31] Chiesa, 2005. "Using Hydrogen as a Gas Turbine Fuel", P. Chiesa and G. Lozza, *ASME Journal of Engineering for Gas Turbines and Power*, 127(1), pp. 73–81.

[32] M. Gazzani, P. Chiesa, E. Martelli, S. Sigali, and I. Brunetti, 2014. "Using Hydrogen as Gas Turbine Fuel: Premixed Versus Diffusive Flame Combustors (2014)", *ASME Journal of Engineering for Gas Turbines and Power*, **136**(5), pp. 051504

[33] E. Martelli, T.G. Kreutz, M. Carbo, S. Consonni, and D. Jansen, 2011. "Shell Coal IGCCs with Carbon Capture: Conventional Gas Quench vs. Innovative Configurations", *Applied Energy* **88** 3978–3989.

[34] GTW 2016. "Gas Turbine World 2016-17 Handbook", Vol. 32, Pequot Publishing Inc., Fairfield, CT.

[35] C. Elsido, E. Martelli, and T. Kreutz, 2016. "Heat Integration, Heat Exchanger Network Synthesis and Heat Recovery Steam Cycle Optimization for a CBTLE Demonstration Plant", Final report for DOE/NETL Project #DE-FE0023697.

[36] C. Elsido, E. Martelli, and T. Kreutz, 2019. "Heat integration and heat recovery steam cycle optimization for a low-carbon lignite/biomass-to-jet fuel demonstration project", *Applied Energy* **239**, 1322-1342. doi.org/10.1016/j.apenergy.2019.01.221

[37] C. Chen, 2016. Personal communication with Chao Chen, Southern Company Services, 30 Aug. - 21 Sept.

[38] M.J. Turner, and L.L. Pinkerton, 2013. "Quality Guidelines for Energy System Studies: Capital Cost Scaling Methodology", DOE/NETL-341/013113, National Energy Technology Laboratory.

[39] CECPI, 2020. *Chemical Engineering*, http://www.che.com/pci/.

[40] W.M. Vatavuk, 2002. "Updating the CE plant cost index", *Chemical Engineering*, pp. 62–70.

[41] C. Greig, A. Garnett, J. Oesch, and S. Smart, 2014. "Guidelines for Scoping and Estimating Early Mover CCS Projects", Milestone 5 Final Report, The University of Queensland.

[42] T. Kreutz, R. Williams, S. Consonni, and P. Chiesa, 2005. "Coproduction of Hydrogen, Electricity, and CO_2 from Coal with Commercially Ready Technology. Part B: Economic Analysis", *International Journal of Hydrogen Energy* **30**, 769–784.

[43] EPRI, 1993. "TAG – Technical Assessment Guide (Electric Supply)", Electric Power Research Institute, Report TR-102275, Vol. 1 Rev. 7, Paolo Alto, CA.

[44] E. Rubin, J. Davison, and H. Herzog, 2015. "The cost of CO_2 capture and storage", *International Journal of GHG Control* **40** 378-400.

[45] G. Haarlemmer, G. Boissonnet, E. Peduzzi, and P. Setiera, 2014. "Investment and production costs of synthetic fuels – A literature survey", *Energy*, **66**, 667-676.

[46] E.O. Oluyede, and J.N. Phillips, 2007. "Fundamental impact of firing syngas in gas turbines", Proceedings of ASME Turbo Expo 2007: Power for Land, Sea and Air, Vol. GT2007-27385.

[47] F. Maréchal, and B. Kalitventzeff, 1998. "Process integration: Selection of the optimal utility system", *Computers & Chemical Engineering*, S149-S156.

[48] F. Maréchal, and B. Kalitventzeff, 1999. "Targeting the optimal integration of steam networks: Mathematical tools and methodology", *Computers and Chemical Engineering*, S133-S136.

[49] C. Elsido, A. Mian, and E. Martelli, 2017. "A systematic methodology for the techno-economic optimization of Organic Rankine Cycles", *Energy Procedia*, **129**, 26-33.

[50] E. Martelli, C. Elsido, A. Mian, and F. Marechal, 2017. "MINLP model and two-stage algorithm for the simultaneous synthesis of heat exchanger networks, utility systems and heat recovery cycles", *Computers and Chemical Engineering,* **106**, 663-689.

[51] C. Elsido, E. Martelli, and I.E. Grossmann, 2019. "A Bilevel Decomposition Method for the Simultaneous Heat Integration and Synthesis of Steam/Organic Rankine Cycles", *Computers & Chemical Engineering*, **128**, 228-145.

[52] NETL, 2007. "Cost and Performance Comparison Baseline for Fossil Energy Power Plants, Volume 1: Bituminous Coal and Natural Gas to Electricity", DOE/NETL-401/053106, Final Report.

[53] D.G. Watts, and D.W. Bacon, 1974. “Using an Hyperbola as a Transition Model to Fit Two-Regime Straight-Line Data”, *Technometrics*, **16**(3), 369-373.